

This discussion paper is/has been under review for the journal *Atmospheric Chemistry and Physics (ACP)*. Please refer to the corresponding final paper in *ACP* if available.

**A comparison of
water uptake**

L. Xu et al.

A comparison of water uptake by aerosols using two thermodynamic models

L. Xu¹, J. E. Penner¹, S. Metzger², and J. Lelieveld²

¹Department of Atmospheric, Oceanic and Space Science, University of Michigan, Ann Arbor, Michigan, USA

²Max Planck Institute for Chemistry, Mainz, Germany

Received: 31 March 2009 – Accepted: 3 April 2009 – Published: 16 April 2009

Correspondence to: L. Xu (lixum@umich.edu)

Published by Copernicus Publications on behalf of the European Geosciences Union.

Title Page

Abstract

Introduction

Conclusions

References

Tables

Figures

◀

▶

◀

▶

Back

Close

Full Screen / Esc

Printer-friendly Version

Interactive Discussion



Abstract

A comprehensive comparison between two aerosol thermodynamic equilibrium models used in chemistry-climate simulations, EQUISOLV II and EQSAM3, is conducted for various relative humidities and chemical compositions. Our results show that the concentration of total particulate matter as well as the associated aerosol liquid water content predicted by these two models is comparable for all conditions, which is important for radiative forcing estimates. The normalized absolute difference in the concentration of total particulate matter is 6% on average for all 200 conditions studied, leading to a regression coefficient of about 0.8 for the water associated with the aerosol between these two models. Relatively large discrepancies occur, however, at high ammonium, low nitrate/sodium concentrations at low and medium relative humidities ($RH < 60\text{--}70\%$), which is analyzed and discussed in detail. In addition, the prediction of the partitioning of ammonium and nitrate is investigated under realistic atmospheric conditions. The data collected during the Mediterranean Intensive Oxidant Study (MINOS) campaign are simulated using both models. The results show that both models can reproduce the concentration of total particulate matter for 90% of the time within a factor of 2, while the predicted concentration of aerosol water by these two models is significantly correlated. The largest difference exists near RH's of 70–80% which is the RH range for the transition of mixed ammonium salts from the solid to the liquid phase.

1 Introduction

Atmospheric aerosols are important as they affect human health, air quality, visibility as well as climate change. The aerosols impact the earth's radiation balance directly through reflecting and absorbing incoming solar radiation back to space and indirectly through changing cloud microphysical properties by acting as cloud condensation nuclei. Accurate methods for predicting atmospheric aerosol composition must be devel-

A comparison of water uptake

L. Xu et al.

Title Page

Abstract

Introduction

Conclusions

References

Tables

Figures

◀

▶

◀

▶

Back

Close

Full Screen / Esc

Printer-friendly Version

Interactive Discussion



**A comparison of
water uptake**

L. Xu et al.

Title Page

Abstract

Introduction

Conclusions

References

Tables

Figures

◀

▶

◀

▶

Back

Close

Full Screen / Esc

Printer-friendly Version

Interactive Discussion



oped in order to better quantify these effects and to understand the underlying physical and chemical processes. Sulfate, nitrate, ammonium, chloride and sodium are among the most important inorganic aerosol species in the atmosphere. Their compounds can be hygroscopic and absorb water under almost all ambient environmental conditions.

5 The uptake of water alters the aerosol size, and causes water to become the constituent with the largest atmospheric aerosol mass, especially when the aerosols grow into fog, haze or clouds (Metzger and Lelieveld, 2007). The uptake of water impacts the wavelength dependent refractive indices, since the refractive index of water is lower than those of other aerosol species. Thus, water plays a significant role in determining
10 the aerosol properties and the radiative forcing of aerosols.

Penner et al. (1998) showed that increasing the RH from 90% to 99% increases the calculated aerosol direct radiative forcing by 50%. Adams et al. (1999) also showed that the amount of water taken up by the aerosol above 95% relative humidity (RH) could increase the total aerosol radiative forcing by about 60%. In a sensitivity study
15 of the direct forcing to various parameters, Pilinis et al. (1995) found that the aerosol radiative forcing is most sensitive to changes in relative humidity and the corresponding water content of the aerosol. In addition, the water content of the aerosol is strongly dependent on the chemical composition of the aerosol particles. In the atmosphere, semivolatile species such as $\text{HNO}_3(\text{g})$ and $\text{NH}_3(\text{g})$ can condense onto nonvolatile sulfate particles to form ionic particles of sulfate (SO_4^{2-}), nitrate (NO_3^-), ammonium (NH_4^+)
20 and protons (H^+) that take up the surrounding water concurrently. This process leads directly to the hygroscopic growth of aerosols. In addition, nitrate and ammonium aerosols can affect tropospheric chemistry by providing additional particle surface for scattering incoming solar radiation (Liao et al., 2003) and further perturbing photochemical oxidant production via altering photolysis frequencies. Thus, in order to
25 better represent the effects of aerosol particles on radiative forcing, the prediction of the partitioning of the volatile inorganic aerosol components between the gas and aerosol phases (ammonia and ammonium, nitric acid and nitrate, etc.) and the aerosol associated water is of great importance in the development of climate models.

**A comparison of
water uptake**

L. Xu et al.

[Title Page](#)[Abstract](#)[Introduction](#)[Conclusions](#)[References](#)[Tables](#)[Figures](#)[I◀](#)[▶I](#)[◀](#)[▶](#)[Back](#)[Close](#)[Full Screen / Esc](#)[Printer-friendly Version](#)[Interactive Discussion](#)

In the past two decades, many thermodynamic equilibrium models have been developed to predict the phase partitioning of multi-component aerosols and their gas-phase precursors in the atmosphere, for instance, EQUIL (Bassett and Seinfeld, 1983), KEQUIL (Bassett and Seinfeld, 1984), MARS (Saxena et al., 1986), SEQUILIB (Pilinis and Seinfeld, 1987), SCAPE and SCAPE2 (Kim et al., 1993a,b; Kim and Seinfeld, 1995; Meng et al., 1995), EQUISOLV and EQUISOLV II (Jacobson et al., 1996; Jacobson, 1999), AIM and AIM2 (Wexler and Seinfeld, 1990, 1991; Clegg et al., 1992, 1994, 1995, 1998a,b; Wexler and Clegg, 2002), ISORROPIA and ISORROPIA II (Nenes et al., 1998, 1999; Fountoukis and Nenes, 2007), GFEMN (Ansari and Pandis, 1999a,b), EQSAM, EQSAM2 and EQSAM3 (Metzger et al., 2002; Metzger et al., 2006; Metzger and Lelieveld, 2007), HETV (Makar et al., 2003), ADDEM (Topping et al., 2005), MESA (Zaveri et al., 2005) and UHAERO (Amundson et al., 2006). Most equilibrium models are computationally expensive since they require iteration in order to reach equilibrium, including EQUISOLV II which has been adopted in the current version of the UMICH-IMPACT-nitrate model (Feng and Penner, 2007). However, both accuracy and high computational efficiency are essential objectives in the development of thermodynamic equilibrium models for chemical transport calculations.

In this study, we conduct a comprehensive comparison for various relative humidities and chemical compositions between EQUISOLV II, one of the most reliable and widely used equilibrium models, and EQSAM3 which is based on a new analytical concept that strongly improves computational efficiency and flexibility regarding the large number of aerosol species that can be considered (currently 100 compounds). In addition, we evaluate the performance of these two models under realistic atmospheric conditions during the Mediterranean Intensive Oxidant Study (MINOS) campaign in Crete in the period 27 July to 25 August 2001 (Lelieveld et al., 2002; Metzger et al., 2006; Salisbury et al., 2003). Our objectives are to gain an understanding of the similarities and differences between these two models for representation of the gas/liquid/solid partitioning of the aerosols under various thermodynamic regimes and recommend further improvements.

A description of EQUISOLV II and EQSAM3 is presented in Sect. 2, followed by a comprehensive comparison of the simulation results from 20 different sets of initial compositions in the Sect. 3. A brief description of the MINOS campaign and a comparison of the model simulations and the observations during this campaign are presented in the Sect. 4. Section 5 presents a discussion and our conclusions.

2 Description of the two thermodynamic equilibrium models

A comparison of the methods used as well as the system solved in EQUISOLV II and EQSAM3 is listed in Table 1. In EQUISOLV II, the equilibrium concentrations of each species are calculated by numerically solving the equilibrium equation for each species separately, accounting for each chemical reaction. The equation for each species is solved in turn and the resulting concentration is used to solve the remaining equations. This sequence is repeated in an iterative manner until the concentrations of all species converge. EQUISOLV II is positive-definite, mass-conserving, and charge-conserving at any point along the iteration procedure (Jacobson, 1999). Bromley's mixing rule (Bromley, 1973) is used to calculate the mean mixed activity coefficients while the mean binary activity coefficient of an electrolyte is parameterized using a number of measurements (Table B.9, Jacobson, 2005) and Pitzer's method (Pitzer and Mayorga, 1973) at 298.15 K. Harned and Owen's (1958) method is adopted to account for the temperature dependency of mean binary solute activity coefficients. The aerosol water content at equilibrium is determined using the Zdanovskii-Stokes-Robinson (ZSR) method (Stokes and Robinson, 1966), by considering the deliquescence relative humidity (DRH) and the crystallization relative humidity (CRH) for single solutes in binary or multi-component mixture (Jacobson, 1999) with temperature dependent but tabulated DRH and CRH. The advantage of EQUISOLV II is that its open architecture makes it easy to incorporate new reactions and species but the shortcoming is that because of the general nature of the solution algorithm it is computationally quite slow even though the analytical equilibrium iteration (AEI) method adopted in EQUISOLV II

A comparison of water uptake

L. Xu et al.

Title Page

Abstract

Introduction

Conclusions

References

Tables

Figures

◀

▶

◀

▶

Back

Close

Full Screen / Esc

Printer-friendly Version

Interactive Discussion



resulted in a speed up of 13–48 times that of an older version of EQUISOLV (Jacobson, 1999).

EQSAM3 is the first solubility-based thermodynamic gas/aerosol equilibrium model (Metzger and Lelieveld, 2007). In contrast to EQUISOLV II and all other thermodynamic gas/aerosol equilibrium models, no iterations are required to solve the entire set of equilibrium reactions and the gas-liquid-solid partitioning. Within EQSAM3, all relevant non-ideal solution properties such as aerosol activities (including activity coefficients, aerosol water and the DRH and CRH of either binary or multi-component aerosol mixtures) are only analytical functions of the solubility of the chemical compounds at a specific RH and temperature. Therefore, EQSAM3 is, similarly as EQSAM and EQSAM2, up to three orders of magnitude more computationally efficient than the current state-of-the-art gas/aerosol equilibrium models as already shown by Metzger et al. (2002).

Another advantage of EQSAM3 is that there are many options that easily allow the control of its complexity. As one example, the neutralization reaction order can be either determined based on the solutes solubility via temperature dependent DRH/CRH of single solutes in binary or mixed solutions, or prescribed according to the Hofmeister series (Metzger and Lelieveld, 2007) that accounts for the degree to which ions bind water (i.e., the so-called salting-out effect). The former neutralization order is automatically determined given the temperature and the solubility of the electrolytes. The electrolyte with a lower solubility is allowed to precipitate out from the solution system at relatively high RH so that the associated ions are bound and are not available for further reactions. Then the partitioning between solid and liquid phase can be computed based on the DRH/CRH of the single solutes in the mixed solution. The concentration of residual gases can be deduced according to the conserved mass. On the other hand, if the reaction order is prescribed, it is assumed that the precipitation of neutralized compounds follows the ability of the ions of the single solutes to neutralize the mixture, in which the ions to the left are neutralized first preferentially:

For anions: $\text{SO}_4^{2-} > \text{HSO}_4^- > \text{NO}_3^- > \text{Cl}^- > \text{CO}_3^{2-}$

A comparison of water uptake

L. Xu et al.

[Title Page](#)[Abstract](#)[Introduction](#)[Conclusions](#)[References](#)[Tables](#)[Figures](#)[◀](#)[▶](#)[◀](#)[▶](#)[Back](#)[Close](#)[Full Screen / Esc](#)[Printer-friendly Version](#)[Interactive Discussion](#)

**A comparison of
water uptake**

L. Xu et al.

Title Page

Abstract

Introduction

Conclusions

References

Tables

Figures

◀

▶

◀

▶

Back

Close

Full Screen / Esc

Printer-friendly Version

Interactive Discussion



For cations: $\text{Mg}^{2+} > \text{Ca}^{2+} > \text{Na}^+ > \text{K}^+ > \text{NH}_4^+ > \text{H}^+$.

This increases the effective concentration of the remaining ions so that they precipitate if their DRH/CRH is reached, e.g. in case of decreasing RH. Since the DRH/CRH dependent neutralization order needs further evaluation, we utilize the prescribed neutralization order based on the Hofmeister series for this comparison. A brief inter-comparison between these two neutralization orders will be presented in the Sect. 3.

Common to both thermodynamic models is that they consider the so-called hysteresis loop, by which atmospheric aerosols take up water when solids deliquesce in case the RH increase above the DRH of individual solid compounds (i.e., following the lower bound of the hysteresis loop), while aerosol water evaporates until crystallization occurs at the CRH when the ambient relative humidity decreases (i.e., following the upper bound of the hysteresis loop). In the latter case, an electrolyte is allowed to form solids which precipitate out from the solution if the RH is below its deliquescence relative humidity (DRH), whereas the electrolyte solid is not allowed to form when the RH is above the electrolyte's DRH, even if the electrolyte is in a multi-component mixture (Jacobson, 1999; Metzger and Lelieveld, 2007). On the other hand, if the ambient RH is decreasing, water evaporates from the aerosol particles which increase the solute concentration. At the DRH, the solution remains supersaturated and is not allowed to crystallize until the crystallization relative humidity (CRH) is reached. The aerosol particle is considered dry when the RH drops below the lowest CRH of the solute present in the actual solution.

Since aerosol water depends on both the composition of the solution and the solute concentration, an iterative procedure is usually required to solve the gas-liquid-solid aerosol partitioning, as it is the case for EQUISOLV II. However, since the RH fixes the water activity of atmospheric aerosols in equilibrium with the ambient air, the new solubility method of Metzger and Lelieveld (2007) applied in EQSAM3 is sufficient to calculate the water uptake of atmospheric aerosol particles analytically.

3 Comparison of simulation results

In order to compare these two models under similar conditions, some modifications were necessary. In EQUISOLV II, we switched off the chemical reaction involved in the formation of solid $(\text{NH}_4)_3\text{H}(\text{SO}_4)_2$ (letovicite), since EQSAM3 excludes the formation of letovicite. As discussed in Sect. 2, the derived DRH in EQSAM3 depends only on the solubility of the solute given the temperature and ambient RH, so we deduced a modified solubility for all the chemical compounds given the DRHs used in EQUISOLV II such that the calculated DRHs in EQSAM3 (according to the Eq. 21, Metzger and Lelieveld, 2007) are exactly the same as those prescribed in EQUISOLV II. The derived solubilities of the major solid compounds and their DRHs are listed in the Table 2. The DRH of Na_2SO_4 and in particular of NaHSO_4 calculated using the solubility from the Handbook of Chemistry and Physics is at variance with the value used in EQUISOLV II.

Table 3 lists a set of 20 different initial conditions similar to the 20 cases in the thermodynamic model inter-comparison of Zhang et al. (2000), but with the addition of initial conditions for the crustal elements (K^+ , Ca^{2+} , and Mg^{2+}). Ansari and Pandis (1999a) show that the inclusion of crustal species could improve the agreement of the prediction from the model to measurements by up to 15% in locations where crustal elements are of significance and Jacobson (1999) found that the presence of the Ca^{2+} and Mg^{2+} significantly affected the prediction of nitrate and ammonium in more polluted locations, such as Los Angeles. Metzger et al. (2006) also show that the consideration of mineral cations is important to balance aerosol ammonium. Hence, it is essential to account for the impacts of crustal species on the prediction of particulate ammonium and nitrate in general. We conducted 10 simulations for each initial condition, by using 10 different RH varying from 10% to 95% at a temperature of 298.15 K. For these 20 initial conditions, the concentration of total sulfate is fixed at $20 \mu\text{g m}^{-3}$. Because H_2SO_4 has a very low vapor pressure, its gas phase concentration is negligible, so its concentration is used as a reference for the other species. Thus, we define the initial chemical concentrations of the other compounds according to seven dimen-

A comparison of water uptake

L. Xu et al.

[Title Page](#)[Abstract](#)[Introduction](#)[Conclusions](#)[References](#)[Tables](#)[Figures](#)[◀](#)[▶](#)[◀](#)[▶](#)[Back](#)[Close](#)[Full Screen / Esc](#)[Printer-friendly Version](#)[Interactive Discussion](#)

A comparison of water uptake

L. Xu et al.

Title Page

Abstract

Introduction

Conclusions

References

Tables

Figures

◀

▶

◀

▶

Back

Close

Full Screen / Esc

Printer-friendly Version

Interactive Discussion



sionless ratios with respect to total sulfate: the molar ratio of total ammonium (i.e., $t_{\text{NH}_4} = n_{\text{NH}_4^+(\text{p})} + n_{\text{NH}_3(\text{g})}$) to total sulfate (referred to as $\frac{t_{\text{NH}_4}}{t_{\text{SO}_4}}$), the molar ratio of total nitrate (i.e., $t_{\text{NO}_3} = n_{\text{NO}_3^-(\text{p})} + n_{\text{HNO}_3(\text{g})}$) to total sulfate (referred to as $\frac{t_{\text{NO}_3}}{t_{\text{SO}_4}}$), the molar ratio of total sodium chloride to total sulfate (referred to as $\frac{t_{\text{NaCl}}}{t_{\text{SO}_4}}$), the molar ratio of total potassium to total sulfate (referred to as $\frac{t_{\text{K}}}{t_{\text{SO}_4}}$), the molar ratio of total calcium to total sulfate (referred to as $\frac{t_{\text{Ca}}}{t_{\text{SO}_4}}$), the molar ratio of total magnesium to total sulfate (referred to as $\frac{t_{\text{Mg}}}{t_{\text{SO}_4}}$) and the molar ratio of total cation species to total sulfate (referred to as $\frac{t_{\text{CAT}}}{t_{\text{SO}_4}}$), where t_{CAT} is defined as:

$$t_{\text{CAT}} = n_{\text{NH}_4^+} + n_{\text{Na}^+} + n_{\text{K}^+} + 2n_{\text{Ca}^{2+}} + 2n_{\text{Mg}^{2+}} .$$

The dominant composition potentially present in the system is determined by the ratio $\frac{t_{\text{CAT}}}{t_{\text{SO}_4}}$. If $\frac{t_{\text{CAT}}}{t_{\text{SO}_4}} < 2$, all available cation species react with the sulfate and the system contains excess sulfate and is called the sulfate rich regime. If $\frac{t_{\text{CAT}}}{t_{\text{SO}_4}} = 2$, all available cation species are just sufficient to neutralize the sulfate present in the system and this is called the sulfate neutral regime. If $\frac{t_{\text{CAT}}}{t_{\text{SO}_4}} > 2$, the available sulfate in the system is not enough to neutralize the cation species and this is called the sulfate poor regime. For the 20 sets of conditions, conditions 1–5 are in the sulfate rich regime, conditions 6–10 are sulfate neutral, and conditions 11–20 are sulfate poor. Note that we also include some of the same cases in each of these three regimes that were included in the inter-comparison of Zhang et al. (2000) so that a direct comparison of our results with the results of that study can be made. Simulations are carried out under the assumption that aerosols lie on the deliquescence branch. A sensitivity test to explore differences when using efflorescence will be investigated in Sect. 4.

Figure 1 shows scatter plots of the concentration of aerosol water, total particulate matter, nitrate, ammonium, chloride, and potential of hydrogen labeled as $\text{H}_2\text{O}(\text{aq})$,

PM, $[\text{NO}_3^-]_p$, $[\text{NH}_4^+]_p$, $[\text{Cl}^-]_p$, and pH predicted by EQSAM3 and EQUISOLV II under all 200 simulation conditions specified in Table 3. The solid black lines are the 1:2, 1:1 and 2:1 lines. The prescribed neutralization order specified by the Hofmeister series in EQSAM3 was adopted in this figure.

3.1 Aerosol water

For all conditions, the aerosol water $\text{H}_2\text{O}(\text{aq})$ predicted by EQSAM3 is close to or less than that predicted by EQUISOLV II except in sulfate rich conditions where EQSAM3 overestimates the aerosol water predicted by EQUISOLV II. For most cases, the difference is well within a factor of 2, and on average EQSAM3 underestimates aerosol water by 29% for the sulfate poor and neutral conditions, due to the differences in predicting bi-sulfates in the sulfate neutral regime that were not determined within EQSAM3 and the difference in predicting the amount of NH_4NO_3 and NH_4Cl in the sulfate poor regime. Table 4 gives the relative difference and linear regression slope along with its 95% confidence interval (CI) of aerosol water and total particulate matter between EQSAM3 and EQUISOLV II for three sulfate regimes at 298.15 K under all RH conditions shown in Fig. 1. “Rich” stands for the sulfate rich regime (i.e., cases 1–5); “Neutral” stands for the sulfate neutral regime (i.e., cases 6–10); “Poor” stands for the sulfate poor regime (i.e., cases 11–20); “All” stands for the conditions including all three sulfate regimes. Here we exclude values in our statistical table and the linear regression calculation, if the aerosol water predicted by two models is less than $1.0 \mu\text{g m}^{-3}$. The relative difference is defined as $\frac{\text{EQ3}-\text{EQ2}}{\text{EQ2}} \times 100\%$, where EQ3 and EQ2 stand for EQSAM3 and EQUISOLV II, respectively. Overall, the slope of regression line between the aerosol water predicted by EQUISOLV II and that predicted by EQSAM3 is 0.79 with a 95% CI of 0.03 for all 200 conditions shown in Table 3. For the sulfate rich regime, the slope is 0.91 with a 95% CI of 0.05 while it is 0.75 with a CI of 0.07 for the sulfate neutral regime and 0.79 with a CI of 0.06 for the sulfate poor regime. The discrepancy in the aerosol water between these two models is either due to differences in the prediction of the partitioning of volatile species (i.e., ammonia and ammonium,

A comparison of water uptake

L. Xu et al.

[Title Page](#)[Abstract](#)[Introduction](#)[Conclusions](#)[References](#)[Tables](#)[Figures](#)[◀](#)[▶](#)[◀](#)[▶](#)[Back](#)[Close](#)[Full Screen / Esc](#)[Printer-friendly Version](#)[Interactive Discussion](#)

nitric acid and nitrate, etc.) or due to the different treatment of bi-sulfates by these two models, which affects the gas/liquid-solid partitioning and will be discussed in more detail later.

3.2 Total particulate matter

As shown in Table 4, EQSAM3 slightly overestimates total particulate matter (PM) by 6% compared to EQUISOLV II for all 200 simulations shown in the Table 3 when the prescribed neutralization order was adopted. The slope of the linear regression line between the PM predicted by EQUISOLV II and that predicted by EQSAM3 is up to 0.9 with a 95% CI of 0.04 for all 200 conditions, which indicates a good agreement between the two models on the prediction of PM. At the sulfate rich and neutral regimes, EQSAM3 predicted PM close to or a little less than EQUISOLV II by about 3% while it overestimates PM by 15% as the sulfate is poor. Table 5 shows the total particulate matter predicted by EQSAM3 and EQUISOLV II at 298.15 K and 30% RH for all 20 conditions and their relative difference. The total PM predicted by EQSAM3 is similar to that of EQUISOLV II for almost all conditions except for the sulfate poor conditions, especially at the conditions with high ammonium ($\frac{t_{\text{NH}_4}}{t_{\text{SO}_4}}=4.0$) and low sodium ($\frac{t_{\text{NaCl}}}{t_{\text{SO}_4}}=0.5$). Under these conditions EQSAM3 predicts up to 50% more total particulate than EQUISOLV II (e.g., case 14) because more ammonium nitrate is predicted in EQSAM3 than in EQUISOLV II for this condition. The normalized relative difference is defined the same as that in Table 4. The value in parentheses in the EQUISOLV II column in Table 5 is the PM concentration predicted by EQUISOLV II presented in Zhang et al. (2000). The value in parentheses in the EQSAM3 and the relative difference column refer to the DRH-dependent neutralization order of EQSAM3. Notice that there is a slight difference with respect to the PM concentration predicted in EQUISOLV II in this study compared to that in Zhang et al. (2000) because we switched off the formation of letovicite in order to match the solid components predicted in EQSAM3. At RH 30%, the PM predicted by EQSAM3 is about 14% higher than that predicted by EQUISOLV

A comparison of water uptake

L. Xu et al.

Title Page

Abstract

Introduction

Conclusions

References

Tables

Figures

◀

▶

◀

▶

Back

Close

Full Screen / Esc

Printer-friendly Version

Interactive Discussion



**A comparison of
water uptake**

L. Xu et al.

Title Page

Abstract

Introduction

Conclusions

References

Tables

Figures

◀

▶

◀

▶

Back

Close

Full Screen / Esc

Printer-friendly Version

Interactive Discussion



II for all conditions when using the prescribed reaction order. For the sulfate rich and neutral regime, EQSAM3 slightly underestimates the total particulate matter by about 3% compared with that predicted by EQUISOLV II, which is consistent with what we found in Table 4. The largest discrepancy occurs in the sulfate poor regime with an average overestimation of about 30% and one case with a difference as large as 50%.

When using the DRH-dependent neutralization order, the total PM predicted by EQSAM3 is overestimated by about 53% compared to that in EQUISOLV II with the largest difference being 74% at RH 30% given in the Table 5. Our comparison indicates that there is better agreement between EQSAM3 and EQUISOLV II using the prescribed neutralization order in EQSAM3. Hence, we choose the prescribed neutralization order hereafter for further evaluation and discuss the potential likelihood in the discussion section.

3.3 Particulate nitrate

For most cases in the sulfate poor regime, the particulate nitrate concentrations predicted by both models agree except at low RH. At RH values below 60–70%, gaseous ammonia is preferred in EQUISOLV II while EQSAM3 partitions more ammonia to the particulate form, which increases the partitioning of nitric acid to the particulate form. The largest discrepancy in the prediction of the particulate nitrate between EQSAM3 and EQUISOLV II occurs at high ammonium ($\frac{t_{\text{NH}_4}}{t_{\text{SO}_4}}=4.0$), low nitrate ($\frac{t_{\text{NO}_3}}{t_{\text{SO}_4}}=1.0$) concentrations and zero or low NaCl ($\frac{t_{\text{NaCl}}}{t_{\text{SO}_4}}=0.5$) loadings (i.e., cases 11, 14, 17 and 19) which result in the largest relative difference in the total PM (42%, 50%, 43% and 37%, respectively) as shown in the Table 5.

The difference in the total PM concentration is much smaller at conditions with high ammonium and low nitrate and high NaCl ($\frac{t_{\text{NaCl}}}{t_{\text{SO}_4}}=2.0$) loadings. For example, the relative difference between these two models drops from 50% to 28% and from 43% to 25% in going from case 14 to case 15 and from case 17 to case 18, respectively. From

A comparison of water uptake

L. Xu et al.

Title Page

Abstract

Introduction

Conclusions

References

Tables

Figures

◀

▶

◀

▶

Back

Close

Full Screen / Esc

Printer-friendly Version

Interactive Discussion



Fig. 3, we see that EQSAM3 predicts the same amount of solid particulate nitrate (i.e., $\text{NH}_4\text{NO}_3(\text{s})$) for both case 14 and case 15. This is in contrast to EQUISOLV II, in which the amount of particulate NO_3^- depends on the amount of sodium. The addition of sodium chloride drives the reaction $\text{NaCl}(\text{s}) + \text{HNO}_3(\text{g}) \rightleftharpoons \text{NaNO}_3(\text{s}) + \text{HCl}(\text{g})$ to the right-hand side and the dissociation of $\text{NaNO}_3(\text{s})$ produces the NO_3^- ion which can bind with NH_4^+ to form $\text{NH}_4\text{NO}_3(\text{s})$, resulting in the increase of nitrate present in the aerosol phase (case 14 vs. case 15) and further enhances the amount of total particulate matter. The similar chemical mechanism holds to the formation of $\text{NH}_4\text{Cl}(\text{s})$ (i.e., case 15 vs. case 14 or case 18 vs. case 17). The relative difference in the total PM concentration between EQSAM3 and EQUISOLV II is reduced in conditions with high ammonium ($\frac{t_{\text{NH}_4}}{t_{\text{SO}_4}} = 4.0$) and high nitrate ($\frac{t_{\text{NO}_3}}{t_{\text{SO}_4}} = 3.0$) but without any sodium chloride present. For example, the relative difference drops from 42% to 20% and from 37% to 19% in going from case 11 to case 12 and from case 19 to case 20, respectively, as a result of differences in the amount of predicted particulate nitrate.

In EQUISOLV II (Jacobson, 2005), a solid electrolyte is allowed to form when the RH is less than its DRH and the product of its reactant ion concentration and mean solute activity coefficient exceeds its solubility product, i.e. the equilibrium coefficient, $K_{\text{eq},i}(T)$. For example, in the reversible reaction $\text{NH}_4\text{NO}_3(\text{s}) \rightleftharpoons \text{NH}_4^+ + \text{NO}_3^-$, the precipitation of ammonium nitrate from the solution phase in EQUISOLV II may occur when

$$m_{\text{NH}_4^+} m_{\text{NO}_3^-} \gamma_{\text{NH}_4^+, \text{NO}_3^-}^2 > K_{\text{eq},i}(T)$$

where the subscript i , differentiates the equilibrium coefficient for this reaction. A solid may also form directly due to the heterogeneous reaction of gases on the surface of a particle. For example, in the reaction $\text{NH}_4\text{NO}_3(\text{s}) \rightleftharpoons \text{NH}_3(\text{g}) + \text{HNO}_3(\text{g})$, a solid will form when $\text{RH} < \text{RHD}$ and

$$p_{\text{NH}_3(\text{g})} p_{\text{HNO}_3(\text{g})} > K_{\text{eq},j}(T)$$

Thus, when the addition of Na^+ occurs, more $\text{NaNO}_3(\text{s})$ forms, and NH_4^+ is able to neutralize SO_4^{2-} rather than NO_3^- , which increases the alkalinity of the system. The

**A comparison of
water uptake**

L. Xu et al.

Title Page

Abstract

Introduction

Conclusions

References

Tables

Figures

I◀

▶I

◀

▶

Back

Close

Full Screen / Esc

Printer-friendly Version

Interactive Discussion



excess $\text{NH}_3(\text{g})$ can further neutralize NO_3^- or Cl^- to form NH_4NO_3 and NH_4Cl , resulting in higher concentrations of particulate nitrate as well as the total PM and liquid water content as shown in case 15 with its high ammonium, nitrate and sodium chloride loadings. When NaCl is not included, the addition of total nitrate to the system increases the vapor pressure of $\text{HNO}_3(\text{g})$ and shifts the reaction of $\text{NH}_4\text{NO}_3(\text{s}) \rightleftharpoons \text{NH}_3(\text{g}) + \text{HNO}_3(\text{g})$ to the left-hand side which increases the formation of solid NH_4NO_3 , leading to higher concentrations of particulate nitrate as shown in case 12.

Similar to EQUISOLV II, a solid electrolyte is allowed to form in EQSAM3 when the RH is less than its DRH, but before a solid electrolyte precipitates out of the solution the product of the reactant ion concentration must exceed the (temperature-dependent) solubility constant, for non-volatile compounds independent of the mean solute activity coefficient, in contrast to EQUISOLV II. Here, we found that in case the RH is lower than the DRH of nitrate salts, the amount of solid nitrate predicted by EQSAM3 is larger than that from EQUISOLV II. The amount of particulate nitrate in the solid phase at lower RH is hereby determined by the minimum amount of total nitrate and the available cation species in EQSAM3, whereas, in EQUISOLV II, the solid particulate nitrate is calculated by solving the equilibrium reaction equations of the solid compounds individually. However, at the higher RH ($>70\%$), EQUISOLV II predicts higher aerosol nitrate than EQSAM3; most likely because the activity coefficient for NH_4NO_3 in EQUISOLV II is slightly greater than that in EQSAM3 at lower molalities or higher relative humidities as shown in Fig. 2a.

For sulfate rich and neutral regimes, both models predict either zero or a negligible amount of particulate nitrate for low RH ($<60\text{--}70\%$). At higher RH conditions, EQUISOLV II predicts higher particulate nitrate than EQSAM3, as aqueous uptake of HNO_3 (and other gases) is not considered in EQSAM3 – coupling with an aqueous phase chemistry module is foreseen instead. Finally, the deviation of EQSAM3 from EQUISOLV II is negligible for conditions with low nitrate and low ammonium.

3.4 Particulate ammonium

The particulate ammonium predicted by EQSAM3 and EQUISOLV II are in good agreement under most conditions, especially in the sulfate rich and neutral regimes ($\frac{t_{\text{CAT}}}{t_{\text{SO}_4}} < 2$ or $\frac{t_{\text{CAT}}}{t_{\text{SO}_4}} = 2$) in which the sulfate is in excess of the number of cations or is just sufficient to neutralize the number of cations. Thus, all the available ammonium is neutralized by the sulfate and present in the aerosol phase. In sulfate poor conditions, the particulate ammonium in EQSAM3 is within a factor of 2 of that in EQUISOLV II. EQSAM3 predicts a larger amount of particulate ammonium at smaller RH but a smaller amount at higher RH compared to EQUISOLV II. The reason is the same as that discussed above for particulate nitrate under similar conditions. That is because the activity coefficients of NH_4NO_3 and NH_4Cl in EQUISOLV II are higher than those used in EQSAM3 at lower molality (i.e., higher RH). At lower RH, the amount of particulate ammonium is determined in EQSAM3 by the total ammonium as well as the amount of anion species available for neutralization, while that predicted by EQUISOLV II is determined by the temperature-dependent equilibrium constant.

3.5 Particulate chloride

The concentrations of particulate chloride predicted by EQAM3 are in agreement with those predicted by EQUISOLV II in sulfate poor conditions. Under sulfate rich and neutral conditions, the concentration of particulate chloride predicted by both EQSAM3 and EQUISOLV II are negligible. Under sulfate poor conditions, the amount of particulate chloride that forms depends on the amount of NaCl or other crustal species (i.e., K^+ , Ca^{2+} , Mg^{2+}). The presence of metal cations can neutralize sulfate and increase the alkalinity of the system, which allows any excess $\text{NH}_3(\text{g})$ to be neutralized by Cl^- to form NH_4Cl , resulting in a higher concentration of particulate chloride. This is similar to the effects of sodium on the amount of the particulate nitrate.

A comparison of water uptake

L. Xu et al.

Title Page

Abstract

Introduction

Conclusions

References

Tables

Figures

◀

▶

◀

▶

Back

Close

Full Screen / Esc

Printer-friendly Version

Interactive Discussion



3.6 Potential of hydrogen

There is a larger discrepancy between the predictions of potential of hydrogen (pH) in the solution system between these two models for the sulfate rich and neutral regimes. Compared to EQUISOLV II, EQSAM3 overestimates the acidity of the solution system on average under the sulfate neutral condition while the underestimation occurs under the sulfate rich condition. For most cases in the sulfate poor condition, the difference between EQSAM3 and EQUISOLV II is well within a factor of 2.

3.7 Dominant solid PM compounds

Figure 3 shows the concentrations of the dominant solid compounds (i.e., $(\text{NH}_4)_2\text{SO}_4$, NH_4HSO_4 , NH_4NO_3 , NH_4Cl , Na_2SO_4 , NaHSO_4 , NaNO_3 and NaCl) predicted by EQSAM3 and EQUISOLV II at RH 30% and a temperature of 298.15 K. The “other” category in the figure includes all the rest of the solid compounds in the system. In the sulfate rich regime (i.e., cases 1–5), the ammonium ion neutralizes sulfate ion to form NH_4HSO_4 in EQUISOLV II while the formation of $(\text{NH}_4)_2\text{SO}_4$ is dominant in EQSAM3, due to our assumption in the model initialization. The prediction in EQUISOLV II is consistent with the fact that aqueous sulfate mainly dissociates to form one hydrogen ion and one bisulfate ion when sulfate is in excess. The prediction of dominant solid compounds in ISORROPIA II is similar in the sulfate rich regime (Foutoukis and Nenes, 2007). Seinfeld and Pandis (1998) also showed that the particles consist mainly of bisulfate in the sulfuric acid-ammonia-water system for an acidic atmosphere ($\text{TNH}_4/\text{TSO}_4 > 0.5$ and $\text{TNH}_4/\text{TSO}_4 < 1.5$). The preferred composition of the aerosol phase is only ammonium sulfate if there is sufficient ammonia to neutralize the available sulfuric acid in the system. Spann and Richardson (1985) observed that ammonium bisulfate is the preferred composition in mixed ammonium and sulfate particles if the molar ratio of $\frac{t_{\text{NH}_4}}{t_{\text{SO}_4}}$ is between 1.0 and 1.5. The addition of crustal species (i.e., K^+ , Ca^{2+} , Mg^{2+}) allows Na^+ to neutralize the sulfate to form $\text{NaHSO}_4(\text{s})$ and $\text{Na}_2\text{SO}_4(\text{s})$

A comparison of water uptake

L. Xu et al.

Title Page

Abstract

Introduction

Conclusions

References

Tables

Figures

◀

▶

◀

▶

Back

Close

Full Screen / Esc

Printer-friendly Version

Interactive Discussion



**A comparison of
water uptake**

L. Xu et al.

Title Page

Abstract

Introduction

Conclusions

References

Tables

Figures

◀

▶

◀

▶

Back

Close

Full Screen / Esc

Printer-friendly Version

Interactive Discussion



and crustal species stay in the aqueous phase in EQUISOLV II, resulting in an increase in the total solid particulate matter. In contrast, EQSAM3 does not show this behavior because crustal compounds like CaSO_4 with a low solubility practically remain as pure solids over the entire RH range in EQSAM3 (Metzger and Lelieveld, 2007). Therefore, if crustal species are added to the system, which directly form a solid at 30% RH, the solid particulate matter increases; comparing case 3 with case 4 in EQSAM3 in Table 5, while there is a slight decrease in the total particulate matter. The reason is that crustal species preferentially neutralize the anions than does ammonium, so that ammonium is driven out of the aerosol phase, remaining the gas phase $\text{NH}_3(\text{g})$ in cases of excess crustal cations. This further results in less aerosol associated water along with more solid particulate matter and hence a slight decrease in the total PM. In the sulfate neutral regime (i.e., cases 6–10), the total solid particulate matter predicted by EQUISOLV II (which is dominated by sulfate salts mixed with some bisulfate salts) is slightly higher than that in EQSAM3 in which only sulfate salts are predicted. In the sulfate poor regime, EQSAM3 predicts more solid NH_4NO_3 and NH_4Cl than that predicted by EQUISOLV II for almost all the conditions at RH 30%. There is no solid NH_4NO_3 predicted in EQUISOLV II under conditions with high ammonium and low nitrate (e.g., case 11). By adding more total nitrate to the system which increases the vapor pressure of $\text{HNO}_3(\text{g})$, NH_4NO_3 begins to form in EQUISOLV II (i.e., case 12). In EQSAM3, on the other hand, the formation of solid NH_4NO_3 depends only on the solubility of NH_4NO_3 and whether or not ammonium is in excess in the system. Additionally, no solid NH_4Cl forms in EQUISOLV II in case 17. Increasing the ratio $\frac{f_{\text{NaCl}}}{f_{\text{SO}_4}}$ from 0.5 to 2, allows more Na^+ to neutralize SO_4^{2-} , resulting in an increase in the availability of ammonium to bind with NO_3^- and Cl^- to form NH_4NO_3 and NH_4Cl in case 18. Figure 2a shows the mean binary activity coefficients of NH_4NO_3 and NH_4Cl as a function of molality while Fig. 2b shows the predicted molality of several electrolytes at a temperature 298.15 K as a function of water activity. There is some difference in the activity coefficients as well as the molality of the two dominant solid compounds (NH_4NO_3 and NH_4Cl) in EQSAM3 and EQUISOLV II, especially for NH_4Cl . Note that a significant

discrepancy also occurs in the molality of NaHSO_4 . Since no bisulfate solid compound (i.e., NH_4HSO_4 or NaHSO_4) is considered to be predicted in the sulfate rich regime in our set up of EQSAM3, the different treatment of the bi-salts like NaHSO_4 in EQSAM3 and EQUISOLV II is responsible for the model discrepancies in the sulfate rich and neutral regimes.

3.8 Growth factor

Figure 4 shows the relative difference in the growth factor between EQSAM3 and EQUISOLV II as a function of RH at a temperature of 298.15 K. The error bars indicate the range of change in the growth factor for all 20 cases. Here the growth factor is defined as the increase in the particle radius due to the uptake of water, mathematically expressed as

$$\text{GF} = (\rho/\rho_w \times w_{\text{H}_2\text{O}}/\text{PM} + 1)^{1/3}$$

Where GF is the growth factor, ρ is the density of the total aerosol mass including aerosol associated water, ρ_w is the density of liquid water, $w_{\text{H}_2\text{O}}$ is the aerosol water predicted by the model, PM is the total particulate matter. The growth factor predicted by EQSAM3 and EQUISOLV II are in good agreement with a relative difference within 10% except at a RH of 70%. The larger difference at 70% RH is due to a different prediction of the transition state for solid dissociation in the sulfate poor regime. When ammonium is in excess, ammonium sulfate and ammonium nitrate are the dominant solid compounds predicted in both models. EQUISOLV II predicts the multi-stage dissociation of multi-component mixtures by rigorously solving the solid equilibrium reactions at various RH. For example, Fig. 5 in Jacobson et al. (1996) shows that ammonium sulfate and ammonium nitrate dissolve when the RH increases to about 62% and that the liquid water content of the solution increases with an increasing rate of dissolution of nitric acid and ammonia from the gas phase as the RH passes the MDRH. This indicates that the transition of mixed salts composed of ammonium sulfate and ammonium nitrate from the solid phase to the aqueous phase in EQUISOLV II occurs at a RH of

A comparison of water uptake

L. Xu et al.

Title Page

Abstract

Introduction

Conclusions

References

Tables

Figures

◀

▶

◀

▶

Back

Close

Full Screen / Esc

Printer-friendly Version

Interactive Discussion



**A comparison of
water uptake**

L. Xu et al.

around 62%. This agrees with the findings in this study for the mixture of ammonium sulfate and ammonium nitrate, e.g., case 12. In EQUISOLV II, the solid ammonium nitrate starts to dissolve in the solution system at a RH around 60% in case 12. In contrast, for the same initial condition, the transition in EQSAM3 occurred at a RH of around 70% in the simulation, when RH passes the DRH of NH_4NO_3 (i.e., 62%). This affects the aerosol water content, which is predicted to be higher by EQUISOLV II at RH 70% than by EQSAM3, eventually leading to larger difference of growth factors between the two models around RH=70%.

4 Comparison with MINOS observations

The Mediterranean Intensive Oxidant Study (MINOS) was conducted in Crete, Greece, in the summer of 2001 from 28 July till 21 August and included a combination of ground-based measurements (i.e., gases, radiation, and meteorological parameters) observed at Finokalia in the north of Crete (35°N , 25°E) and two aircraft operated from Heraklion airport which performed measurements across the Mediterranean from the surface throughout the troposphere (Lelieveld et al., 2002; Salisbury et al., 2003). This region is characterized by high solar intensity, humid marine air and polluted air from Europe in the summer, so that one of the goals of MINOS was to investigate the role of chemistry and transport processes in the Mediterranean environment in contributing to the high level of air pollutants. The study also offered an opportunity to investigate the partitioning of volatile species (i.e., HNO_3 , NH_3 and HCl) between the gas and the aerosol phase.

Atmospheric HNO_3 and NH_3 were collected by a Cofer sampler with a flow rate 16 L min^{-1} and a sampling step 2–3 h. The concentration of $\text{HNO}_3(\text{g})$ and $\text{NH}_3(\text{g})$ were determined by using ion chromatography with a detection limit for the mean sampling volume of 3 m^3 of 20 pmol mol^{-1} and a precision of about 15%. The bulk aerosol samples were collected by PTFE filters running simultaneously with the Cofer sampler. A total 226 aerosol samples were collected during the period of the campaign. The

[Title Page](#)[Abstract](#)[Introduction](#)[Conclusions](#)[References](#)[Tables](#)[Figures](#)[◀](#)[▶](#)[◀](#)[▶](#)[Back](#)[Close](#)[Full Screen / Esc](#)[Printer-friendly Version](#)[Interactive Discussion](#)

**A comparison of
water uptake**

L. Xu et al.

Title Page

Abstract

Introduction

Conclusions

References

Tables

Figures

◀

▶

◀

▶

Back

Close

Full Screen / Esc

Printer-friendly Version

Interactive Discussion



main anions and cations on the filters were analyzed by ion Chromatography, using a Dionex AS4A-SC column with ASRS-I suppressor in auto-suppression mode of operation for the main anions (i.e., Cl^- , NO_3^- , SO_4^{2-}) while the main cations (i.e., NH_4^+ , Na^+ , K^+ , Mg^{2+} , Ca^{2+}) were analyzed using a CS12-SC column with CSRS-I suppressor. The detection limits for both main anions and cations were around 5 ppb. More details can be found in Kouvarskis and Mihalopoulos (2002).

The measured concentrations of gases (g) and aerosols (p) used as input to the two thermodynamic models include total ammonium ($\text{NH}_3(\text{g})$ and $\text{NH}_4^+(\text{p})$), total nitrate ($\text{HNO}_3(\text{g})$ and $\text{NO}_3^-(\text{p})$), total sulfate ($\text{H}_2\text{SO}_4(\text{g})$ and $\text{SO}_4^{2-}(\text{p})$), total chloride ($\text{HCl}(\text{g})$ and $\text{Cl}^-(\text{p})$), sodium ($\text{Na}^+(\text{p})$), potassium ($\text{K}^+(\text{p})$), calcium ($\text{Ca}^{2+}(\text{p})$), and magnesium ($\text{Mg}^{2+}(\text{p})$). The aerosol precursor gases and aerosol compounds were partitioned between the gas, liquid, or solid aerosol phase by assuming thermodynamic and chemical equilibrium.

The time scale for a particle to reach equilibrium depends on its size, which can range from seconds or minutes for small particles up to days for coarse particles at low relative humidity and low aerosol concentration conditions (Meng and Seinfeld, 1996). Thus, the total ammonium, total nitrate and total chloride used as input to the models is the only the sum of the amount measured in the fine-mode particles ($D < 1.2 \mu\text{m}$) and the gas phase. The measurement sampling time was 2–3 h which is sufficiently long to achieve equilibrium for the fine mode aerosols.

Figure 5a and c show the time series from 29 July till 22 August of aerosol $\text{NH}_4^+(\text{p})$ and gas $\text{NH}_3(\text{g})$ partitioned by EQSAM3 and EQUISOLV II and the total ammonium $t\text{NH}_4$, aerosol $\text{NH}_4^+(\text{p})$ and gas $\text{NH}_3(\text{g})$ from observations, respectively; Fig. 5b and d show a scatter plot between the model predicted $\text{NH}_4^+(\text{p})$ and the observed values for EQSAM3 and EQUISOLV II. The red line is a linear fit of the blue points. Figure 5e–h show similar plots for aerosol $\text{NO}_3^-(\text{p})$. The regression line as well as the goodness of fit parameter (i.e., the square of correlation coefficient) between the model predictions and the observations is given in Fig. 5. Table 6 presents a summary of the comparison between the model predicted and observed concentrations of ammonium, nitrate and

chloride in the gas and aerosol phase for EQSAM3 (referred to as EQ3) and EQUISOLV II (referred to as EQ2) as well as the model predicted concentrations of total particulate matter, solid particulate matter and aerosol associated water.

Generally, the predictions of EQSAM3 and EQUISOLV II are similar for particulate ammonium and gaseous ammonia. Both capture the hourly and diurnal variations of NH_4^+ seen in the observations, although with occasional excursions. Figure 5 shows that both EQSAM3 and EQUISOLV II underestimate particulate ammonium in general, since organic compounds that were measured are omitted here for modeling consistency, in contrast to previous studies (Metzger et al. 2006; Metzger and Lelieveld, 2007). Still, the results shown in Table 6 are with 72% and 68% of the predicted aerosol NH_4^+ concentrations within a factor of 1.5 of the observations for EQSAM3 and EQUISOLV II, respectively, and up to 90% within a factor of 2. EQSAM3 slightly underestimates aerosol NH_4^+ by 3% on average while EQUISOLV II exhibits a somewhat larger underestimation about 25%. However, the comparison of EQSAM3 and EQUISOLV II with observations for aerosol NO_3^- is less favorable. The mean aerosol NO_3^- in EQSAM3 is roughly a factor of 9 higher than the observed mean value but absolutely rather low concentration. This significant overestimation can also be seen in the scatter plot of observed and predicted aerosol NO_3^- for EQSAM3. Most of the total nitrate in EQSAM3 is in the particulate form, which is predicted to be of order of $1 \mu\text{g m}^{-3}$ whereas most of the observations are of order $0.1 \mu\text{g m}^{-3}$. EQUISOLV II on the other hand, does a much better job of representing the partitioning of total nitrate between the gas and aerosol phase, as gaseous nitric acid is favored over aerosol NO_3^- in both the observations and the predictions. As further shown in Table 6, the concentration of gaseous nitric acid in EQUISOLV II is within a factor of 1.5 of the measurements up to 99% of the time. Nevertheless, the mean aerosol NO_3^- from EQUISOLV II is somewhat smaller than the measurements: $0.04 \mu\text{g m}^{-3}$ in comparison to $0.09 \mu\text{g m}^{-3}$. Overall, the partitioning of total nitrate in EQUISOLV II during the MINOS campaign is better than that of EQSAM3. A similar conclusion holds for the partitioning of total chloride. Table 6 shows that 91% of the predictions of EQUISOLV II are within

A comparison of water uptake

L. Xu et al.

Title Page

Abstract

Introduction

Conclusions

References

Tables

Figures

◀

▶

◀

▶

Back

Close

Full Screen / Esc

Printer-friendly Version

Interactive Discussion



**A comparison of
water uptake**

L. Xu et al.

Title Page

Abstract

Introduction

Conclusions

References

Tables

Figures

◀

▶

◀

▶

Back

Close

Full Screen / Esc

Printer-friendly Version

Interactive Discussion



a factor of 1.5 of the observations for gaseous hydrochloric acid, whereas only 62% of the predictions from EQSAM3 are within a factor of 1.5. Notice that the observed concentrations of aerosol nitrate and chloride are very low ($<0.1 \mu\text{g m}^{-3}$) compared to the amounts present in the gas phase. Thus, there is only a small impact of these compounds on the uptake of water. The prediction of the total particulate matter from the models is slightly lower than that of the observations. However, both models are able to reproduce the observations within a factor 2. The performance of EQSAM3 for total particulate matter is better than that of EQUISOLV II with 90% of the predictions within a factor of 1.5 of the observations. EQSAM3 predicts a higher fraction of solid particulate matter (83%) compared to that in EQUISOLV II (61%), which leads to lower aerosol associated water. The average difference in the prediction of liquid water content between EQSAM3 and EQUISOLV II is $-0.64 \mu\text{g m}^{-3}$, and most of this discrepancy occurs at an RH of about 70–80%. This RH is in the range for the solid-to-liquid transition which was discussed in the Sect. 3. Overall, the correlation coefficient between EQUISOLV II and EQSAM3 on the aerosol associated water is about 0.85.

Figure 6 shows the absolute difference between the predictions of the particulate nitrate concentrations from EQSAM3 and EQUISOLV II and the observations as the function of temperature, relative humidity, sulfate concentration, and the molar ratio of total ammonium to total sulfate. Both EQSAM3 and EQUISOLV II show large discrepancies with observations at low temperatures and high relative humidities. EQUISOLV II slightly underestimates particulate NO_3^- for almost all conditions but some over-predictions occur at lower temperatures, higher relative humidities, and sulfate poor regimes (molar ratio of $t\text{NH}_4/t\text{SO}_4 > 2.0$). This agrees with findings discussed in Yu et al. (2005). Yu et al. (2005) found that ISORROPIA overpredicts particulate nitrate at the conditions of lower temperature, high RH and sulfate poor regimes in Atlanta while underpredictions occur at high temperature, low RH and sulfate rich conditions (molar ratio of $t\text{NH}_4/t\text{SO}_4 < 2.0$). Moya et al. (2001) suggested that a dynamic instead of an equilibrium model may improve the agreement between the model prediction and observations for particulate nitrate under the conditions with high temperatures and low

RH based on observations collected during the IMADA-AVER field study in Mexico City in 1997. EQUISOLV II is in better agreement with the observations with respect to the prediction of nitrate. EQSAM3 predicts a scattered departure from the observations at both high and low concentrations of sulfate and shows somewhat higher departures at high molar ratios of $t\text{NH}_4$ to $t\text{SO}_4$.

Figure 7 is similar to Fig. 6 but for particulate ammonium. The prediction of ammonium from these two models is similar. The prediction of particulate ammonium seems not as sensitive to temperature and relative humidity as the prediction of particulate nitrate in both EQSAM3 and EQUISOLV II. They have small biases with the observations when the molar ratio of $t\text{NH}_4$ to $t\text{SO}_4$ is less than 2 (in the sulfate rich regime) but have a larger discrepancy with the observations at larger molar ratios of $t\text{NH}_4$ to $t\text{SO}_4$ or higher concentration of SO_4^{2-} .

Ansari and Pandis (2000) found that efflorescence branch concentrations of aerosol nitrate are 11% larger than those of the deliquescence branch at low aerosol nitrate concentrations ($<8 \mu\text{g m}^{-3}$). Here we investigate the biases of the models in this metastable regime. Figure 8 shows a histogram of the model bias in the prediction of aerosol nitrate assuming both the deliquescence and efflorescence branch. The absolute difference between EQSAM3 and the observations in the prediction of aerosol nitrate using the efflorescence branch is similar as that of the deliquescence branch. The average model bias shifts from $0.73 \mu\text{g m}^{-3}$ for deliquescence to $0.79 \mu\text{g m}^{-3}$ for efflorescence. In contrast, in the EQUISOLV II, the model mean bias shifts from a slight underestimation of $-0.05 \mu\text{g m}^{-3}$ for deliquescence to an overestimation of $0.02 \mu\text{g m}^{-3}$ for efflorescence. This indicates that the model mean bias slightly decreases if the efflorescence branch in EQUISOLV II is used while the bias in EQSAM3 is not significantly changed.

A comparison of water uptake

L. Xu et al.

Title Page

Abstract

Introduction

Conclusions

References

Tables

Figures

◀

▶

◀

▶

Back

Close

Full Screen / Esc

Printer-friendly Version

Interactive Discussion



5 Discussion and conclusions

We conducted a comprehensive evaluation of two aerosol thermodynamic equilibrium models EQSAM3 and EQUISOLV II under various RH and composition domains. EQSAM3 and EQUISOLV II predict a similar amount of aerosol water for all conditions, with a statistically significant linear regression slope of about 0.8. The agreement is even better in the sulfate rich regime where the linear regression slope is close to 0.91, so that most of the discrepancy between the two models is in the sulfate neutral and poor regime. Although the prediction of the water associated with aerosols in these two models is generally comparable under most conditions, there are large discrepancies under some conditions, which can be explained by the different treatment/prediction of bi-salts (NH_4HSO_4 , NaHSO_4 , KHSO_4), different prediction of transition state of mixed salts (e.g., the mixture of ammonium sulfate and ammonium nitrate) and the aqueous uptake of HNO_3 , HCl and NH_3 which are not considered here in EQSAM3 as the coupling of EQSAM3 with an aqueous phase chemistry module is foreseen instead.

In general, the PM concentration predicted by these two models is consistent except under conditions with high ammonium and low sodium. EQSAM3 slightly overestimates total particulate matter (PM) by 6% compared to EQUISOLV II for all 200 simulation conditions with a statistically significant linear regression slope of 0.9 with a 95% CI of 0.04. At the sulfate rich and neutral regimes, EQSAM3 predicted PM close to or a little less than EQUISOLV II by about 3% while it overestimates PM by 15% as the sulfate is poor. At a temperature of 298.15 K and an RH of 30%, the normalized absolute difference in the concentration of total PM predicted by the two models is about 14%. The largest discrepancies occur in the sulfate poor regime where the two models differ by 30% on average with the largest difference as high as 50% in some specific cases. This leads to differences in the predicted aerosol water. Overall, the particulate nitrate concentration predicted by two models agree with each other except at the low RH (<60–70%) under most conditions in the sulfate poor regime. Then the formation of solids explains the differences in the particulate concentrations. The ad-

A comparison of water uptake

L. Xu et al.

[Title Page](#)[Abstract](#)[Introduction](#)[Conclusions](#)[References](#)[Tables](#)[Figures](#)[◀](#)[▶](#)[◀](#)[▶](#)[Back](#)[Close](#)[Full Screen / Esc](#)[Printer-friendly Version](#)[Interactive Discussion](#)

dition of sodium chloride increases the prediction of particulate nitrate in EQUISOLV II and decreases the relative difference between the two models. At higher RH (>70%), EQUISOLV II predicts higher aerosol nitrate because of slightly larger activity coefficients for NH_4NO_3 . Similar to particulate nitrate, these two models agree under most conditions for particulate ammonium, especially in the sulfate rich and neutral regimes. EQSAM3 shows some deviation from EQUISOLV II but the difference is within a factor of 2. For particulate chloride, the largest difference in the prediction occurs in the sulfate poor regime since the amount of the aerosol chloride strongly depends on the amount of excess ammonium as the weakest cation. There is a larger discrepancy between the predictions of pH in the solution system between these two models for the sulfate rich and neutral regimes. For most cases in the sulfate poor condition, the difference in pH between EQSAM3 and EQUISOLV II is well within a factor of 2.

By comparing the dominant solid PM compounds predicted by the two models at an RH of 30%, we found that the ammonium ion neutralizes the bisulfate ion to form ammonium bisulfate in EQUISOLV II in the sulfate rich regime, while ammonium sulfate is the dominant species in EQSAM3, related to our assumptions in the model set up. This explains the difference between two models in the sulfate rich and neutral conditions. The difference in the activity coefficients as well as the derived molality of major salts in EQSAM3 contributes slightly to the difference in the gas-liquid-solid partitioning in the sulfate poor condition. Overall, the relative difference of the mass growth factor between EQSAM3 and EQUISOLV II at various RH and at a temperature of 298.15 K is about 5%. The largest difference of around 10% occurs at a RH 70% because of the difference in the transition state predicted by two models at RH around 70%.

A comparison was also conducted using realistic atmospheric conditions. The nitrate and ammonium concentrations during the MINOS campaign were simulated for the summer of 2001 from 28 July till 21 August in Crete, Greece, a location characterized by high solar intensity and polluted air from Europe. Overall, both EQSAM3 and EQUISOLV II underestimate particulate ammonium compared with the observations by 3% and 25% on average. The predictions of particulate nitrate from both models devi-

A comparison of water uptake

L. Xu et al.

[Title Page](#)[Abstract](#)[Introduction](#)[Conclusions](#)[References](#)[Tables](#)[Figures](#)[◀](#)[▶](#)[◀](#)[▶](#)[Back](#)[Close](#)[Full Screen / Esc](#)[Printer-friendly Version](#)[Interactive Discussion](#)

ate significantly from the observations. This is due to the fact that the concentration of total nitrate is very low and most of nitrate is in the gas phase. EQUISOLV II is able to reproduce the gaseous nitric acid to within a factor of 1.5 in 99% of the observations, while only 20% of observations are reproduced to within a factor of 1.5 in EQSAM3.

5 However, because of the very low nitrate concentrations, the impact of this difference on the prediction of total particulate matter as well as aerosol water is minor. Thus, both of models are able to reproduce the observed particulate matter to within a factor of 2 in more than 90% of the observations and the predicted water associated with the aerosol in the two models is strongly correlated with a correlation coefficient 0.85. The
10 largest differences exist at an RH 70–80% which corresponds to the RH near the transition to deliquescence as discussed in Sect. 3. Note that although the concentration of total nitrate during the MINOS campaign is low on average, leading to the discrepancy on the prediction of particulate nitrate between model predictions and observations, better agreement is found at the condition of high nitrate according to our findings in Sect. 2 for the comparison of low and high total nitrate (i.e., cases 11 and 12, cases
15 19 and 20).

Finally, a sensitivity test was carried out in order to evaluate the impacts of temperature, RH, sulfate concentration and ammonium-to-sulfate ratio on the prediction of nitrate and ammonium. We found that both EQSAM3 and EQUISOLV II overpredicts
20 particulate nitrate at lower temperatures, higher RH, and in sulfate poor regime. This is consistent with the findings of the models discussed by Moya et al. (2001) and Yu et al. (2005). As for the prediction of particulate ammonium, it seems not as sensitive to temperature and relative humidity as the prediction of particulate nitrate in both EQSAM3 and EQUISOLV II. They show small biases with the observations when the
25 molar ratio of $t\text{NH}_4$ to $t\text{SO}_4$ is less than 2 (in the sulfate rich regime) but tend to have a larger deviation from the observations at higher molar ratios of $t\text{NH}_4$ to $t\text{SO}_4$ or higher concentration of SO_4^{2-} . The impacts of using the efflorescence branch vs. the deliquescence branch were also evaluated. The model mean bias slightly decreases if the efflorescence branch in EQUISOLV II is used while the bias in EQSAM3 is not

A comparison of water uptake

L. Xu et al.

[Title Page](#)[Abstract](#)[Introduction](#)[Conclusions](#)[References](#)[Tables](#)[Figures](#)[◀](#)[▶](#)[◀](#)[▶](#)[Back](#)[Close](#)[Full Screen / Esc](#)[Printer-friendly Version](#)[Interactive Discussion](#)

significantly changed.

Overall, our results show that the results of EQSAM3 and EQUISOLV II are comparable under most conditions. Because of this and the high computational efficiency of EQSAM3, we recommend to incorporate EQSAM3 into global aerosol models to solve the thermodynamics under chemical equilibrium conditions. The few discrepancies found can be minimized either by the coupling of EQSAM3 with an aqueous phase chemistry module, or choosing different assumptions on the treatment on bi-salts, e.g. similar to EQSAM2 (Metzger et al., 2006). More importantly probably, the assumption that equilibrium is achieved between gas and aerosol phase may be a limiting factor for global scale applications by considering larger aerosol modes, since non-equilibrium situations between gas and aerosol phase might then become pre-dominant for the particulate matter or growth factor predictions. We plan to incorporate EQSAM3 into the IMPACT global aerosol model using the hybrid dynamical solution method (Feng and Penner, 2007) to provide a model inter-comparison under a broader range of conditions.

Acknowledgement. LX and JEP are grateful for the support of the NASA Glory Science Team under grant number NNX08AL83G as well as that from NASA JPL under contract number NM0710973. We thank N. Mihalopoulos and the MINOS measurement group for the gas/aerosol measurements.

References

- Adams, P. J., Seinfeld, J. H., and Koch, D. M.: Global concentration of tropospheric sulfate, nitrate, and ammonium aerosol simulated in a general circulate model, *J. Geophys. Res.*, 104, 13791–13823, 1999.
- Ansari, A. S. and Pandis, S. N.: Prediction of multicomponent inorganic atmospheric aerosol behavior, *Atmos. Environ.*, 33, 745–757, 1999a.
- Ansari, A. S. and Pandis, S. N.: An analysis of four models predicting the partitioning of semivolatile inorganic aerosol components, *Aeros. Sci. Tech.*, 31, 129–153, 1999b.

A comparison of water uptake

L. Xu et al.

Title Page

Abstract

Introduction

Conclusions

References

Tables

Figures

◀

▶

◀

▶

Back

Close

Full Screen / Esc

Printer-friendly Version

Interactive Discussion



**A comparison of
water uptake**

L. Xu et al.

Title Page

Abstract

Introduction

Conclusions

References

Tables

Figures

◀

▶

◀

▶

Back

Close

Full Screen / Esc

Printer-friendly Version

Interactive Discussion



- Ansari, A. S. and Pandis, S. N.: The effect of metastable equilibrium states on the partitioning of nitrate between the gas and aerosol phases, *Atmos. Environ.*, 34, 157–168, 2000.
- Amundson, N. R., Caboussat, A., He, J. W., Martynenko, A. V., Savarin, V. B., Seinfeld, J. H., and Yoo, K. Y.: A new inorganic atmospheric aerosol phase equilibrium model (UHAERO), *Atmos. Chem. Phys.*, 6, 975–992, 2006,
5 <http://www.atmos-chem-phys.net/6/975/2006/>.
- Bassett, M. E. and Seinfeld, J. H.: Atmospheric equilibrium models of sulfate and nitrate aerosol II, Particle size analysis, *Atmos., Environ.*, 18, 1163–1170, 1983.
- Bassett, M. E. and Seinfeld, J. H.: Atmospheric equilibrium models of sulfate and nitrate
10 aerosol, *Atmos. Environ.*, 17, 2238–2252, 1984.
- Bromley, L. A.: Thermodynamic properties of strong electrolytes in aqueous solutions, *Al. Ch. E. Journal* 19, 313–320, 1973.
- Clegg, S. L., Pitzer, K. S., and Brimblecombe, P.: Thermodynamics of multicomponent, miscible, ionic solutions. II. Mixture including unsymmetrical electrolytes, *J. Phys. Chem.*, 96, 9470–9479, 1992.
- 15 Clegg, S. L., Pitzer, K. S., and Brimblecombe, P.: Additions and corrections for their published papers, *J. Phys. Chem.*, 98, P. 1368, 1994.
- Clegg, S. L., Pitzer, K. S. and Brimblecombe, P.: Additions and corrections for their published papers, *J. Phys. Chem.*, 99, p. 6755, 1995.
- 20 Clegg, S. L., Brimblecombe, P., and Wexler, A. S.: A thermodynamic model of the system $H^+ - NH_4^+ - Na^+ - SO_4^{2-} - NO_3^- - Cl^- - H_2O$ at 298.15 K, *J. Phys. Chem.*, 102, 2155–2171, 1998a.
- Clegg, S. L., Brimblecombe, P., and Wexler, A. S.: A thermodynamic model of the system $H^+ - NH_4^+ - Na^+ - SO_4^{2-} - NO_3^- - Cl^- - H_2O$ at tropospheric temperatures, *J. Phys. Chem.*, 102, 2137–2154, 1998b.
- 25 Feng, Y. and Penner, J. E.: Global modeling of nitrate and ammonium: Interaction of aerosols and tropospheric chemistry, *J. Geophys. Res.*, 112, D01304, doi:10.1029/2005JD006404, 2007.
- Fountoukis, C. and Nenes, A.: ISORROPIA II: a computationally efficient thermodynamic equilibrium model for $K^+ - Ca^{2+} - Mg^{2+} - NH_4^+ - Na^+ - SO_4^{2-} - NO_3^- - Cl^- - H_2O$ aerosols, *Atmos. Chem. Phys.*, 7, 4639–4659, 2007,
30 <http://www.atmos-chem-phys.net/7/4639/2007/>.
- Harned, H. S. and Owen, B. B.: *The Physical Chemistry of Electrolyte solutions*, Reinhold, New York, Chap. 8, 1958.

**A comparison of
water uptake**

L. Xu et al.

Title Page

Abstract

Introduction

Conclusions

References

Tables

Figures

◀

▶

◀

▶

Back

Close

Full Screen / Esc

Printer-friendly Version

Interactive Discussion



- Jacobson, M. Z., Tabazadeh, A., and Turco, R.: Simulating equilibrium within aerosols and nonequilibrium between gases and aerosols, *J. Geophys. Res.*, 101(D4), 9079–9091, 1996.
- Jacobson, M. Z.: Studying the effects of calcium and magnesium on size-distributed nitrate and ammonium with EQUISOLV II, *Atmos. Environ.*, 33, 3635–3649, 1999.
- 5 Jacobson, M. Z.: *Fundamentals of Atmospheric Modeling*, Cambridge University Press, 2005.
- Kim, Y. P., Seinfeld, J. H., and Saxena, P.: Atmospheric gas aerosol equilibrium, I: thermodynamic model, *Aerosol Sci. Technol.* 19, 157–181, 1993a.
- Kim, Y. P., Seinfeld, J. H., and Saxena, P.: Atmospheric gas aerosol equilibrium, II: analysis of common approximations and activity coefficient calculation methods, *Aerosol Sci. Technol.*
- 10 19, 182–198, 1993b.
- Kim, Y. P. and Seinfeld, J. H.: Atmospheric gas-aerosol equilibrium III: thermo-dynamics of crustal elements Ca^{2+} , K^+ , and Mg^{2+} , *Aerosol Sci. Technol.*, 22, 93–110, 1995.
- Kouvarakis, G. and Mihalopoulos, N.: Seasonal variation of dimethylsulfide in the gas phase and of methanesulfonate and non-sea-salt sulfate in the aerosol phase measured in the Eastern
- 15 Mediterranean atmosphere, *Atmos. Environ.*, 36, 929–938, 2002.
- Lelieveld, J., Berresheim, H., Borrmann, S., Crutzen, P. J., Dentener, F. J., Fischer, H., Feichter, J., Flatau, P. J., Heland, J., Holzinger, R., Kormann, R., Lawrence, M. G., Levin, Z., Markowicz, K. M., Mihalopoulos, N., Minikin, A., Ramanathan, V., de Reus, M., Roelofs, G. J., Scheeren, H. A., Sciare, J., Schlager, H., Schultz, M., Siegmund, P., Steil, B.,
- 20 Stephanou, E. G., Stier, P., Traub, M., Warneke, C., Williams, J., and Ziereis, H.: Global air pollution crossroads over the Mediterranean, *Science*, 298, 794–799, 2002.
- Liao, H., Adams, P. J., Chung, S. H., Seinfeld, J. H., Mickley, L. J. and Jacob, D. J.: Interactions between tropospheric chemistry and aerosols in a unified general circulation model, *J. Geophys. Res.*, 108(D1), 4001, doi:10.1029/2001JD001260, 2003.
- 25 Markar, P. A., Bouchet, V. S., and Nenes, A.: Inorganic chemistry calculations using HETV – a vectorized solver for the SO_4^{2-} - NO_3^- - NH_4^+ system based on the ISORROPIA algorithms, *Atmos. Environ.*, 37, 2279–2294, doi:10.1016/S1352–2310(03)00074–8.510, 2003.
- Meng, Z., Seinfeld, J. H., Saxena, P., and Kim, Y. P.: Atmospheric gas-aerosol equilibrium, IV: thermodynamics of carbonates, *Aerosol Sci. Technol.*, 23, 131–154, 1995.
- 30 Meng, Z. and Seinfeld, J. H.: Time scales to achieve atmospheric gas-aerosol equilibrium for volatile species, *Atmos. Environ.*, 30, 2889–2900, 1996.
- Metzger, S., Dentener, F. J., Lelieveld, J., and Pandis, S. N.: Gas/aerosol partitioning I: A computationally efficient model, *J. Geophys. Res.*, 107(D16), ACH 16-1-24,

doi:10.1029/2001JD001102, 2002.

Metzger, S., Mihalopoulos, N., and Lelieveld, J.: Importance of mineral cations and organics in gas-aerosol partitioning of reactive nitrogen compounds: case study based on MINOS results, *Atmos. Chem. Phys.*, 6, 2549–2567, 2006,

<http://www.atmos-chem-phys.net/6/2549/2006/>.

Metzger, S. and Lelieveld, J.: Reformulating atmospheric aerosol thermodynamics and hygroscopic growth into fog, haze and clouds, *Atmos. Chem. Phys.*, 7, 3163–3193, 2007,

<http://www.atmos-chem-phys.net/7/3163/2007/>.

Moya, M., Ansari, A. S., and Pandis, S. N.: Partitioning of nitrate and ammonium between the gas and particulate phases during the 1997 IMADA-AVER study in Mexico City, *Atmos. Environ.*, 35, 1791–1804, 2001.

Nenes, A., Pilinis, C., and Pandis, S. N.: ISORROPIA: a new thermodynamic equilibrium model for multiphase multicomponent marine aerosols, *Aquatic Geochem.*, 4, 123–152, 1998.

Nenes, A., Pilinis, C., and Pandis, S. N.: Continued development and testing of a new thermodynamic aerosol module for urban and regional air quality models, *Atmos. Environ.*, 33, 1553–1560, 1999.

Penner, J. E., Chuang, C. C., and Grant, K.: Climate forcing by carbonaceous and sulfate aerosols, *Clim. Dym.*, 14, 839–851, 1998.

Pilinis, C. and Seinfeld, J. H.: Continued development of a general equilibrium model for inorganic multicomponent atmospheric aerosols, *Atmos. Environ.*, 32, 2453–2466, 1997.

Pilinis, C., Pandis, S. N., and Seinfeld, J. H.: Sensitivity of direct climate forcing by atmospheric aerosols to aerosol size and composition, *J. Geophys. Res.*, 100, 18739–18754, 1995.

Pitzer, K. S. and Mayorga, G.: Thermodynamics of electrolytes, II, Activity and osmotic coefficients for strong electrolytes with one or both ions univalent, *J. Phys. Chem.*, 77, 2300–2308, 1973.

Salisbury, G., Williams, J., Holzinger, R., Gros, V., Mihalopoulos, N., Vrekoussis, M., Sarda-Estève, R., Berresheim, H., von Kuhlmann, R., Lawrence, M., and Lelieveld, J.: Ground-based PTR-MS measurements of reactive organic compounds during the MINOS campaign in Crete, July–August 2001, *Atmos. Chem. Phys.*, 3, 925–940, 2003,

<http://www.atmos-chem-phys.net/3/925/2003/>.

Saxena, P., Seigneur, C., Hudischewskyj, A. B., and Seinfeld, J. H.: A comparative study of equilibrium approaches to the chemical characterizations of secondary aerosols, *Atmos. Environ.*, 20, 1471–1484, 1986.

A comparison of water uptake

L. Xu et al.

Title Page

Abstract

Introduction

Conclusions

References

Tables

Figures

◀

▶

◀

▶

Back

Close

Full Screen / Esc

Printer-friendly Version

Interactive Discussion



**A comparison of
water uptake**

L. Xu et al.

Title Page

Abstract

Introduction

Conclusions

References

Tables

Figures

I◀

▶I

◀

▶

Back

Close

Full Screen / Esc

Printer-friendly Version

Interactive Discussion



Seinfeld, J. H. and Pandis, S. N.: Atmospheric Chemistry and Physics: From Air Pollution to Climate Change, John, Wiley & Sons, Inc., 1998.

Spann, J. F. and Richardson, C. B.: Measurement of the water cycle in mixed ammonium acid sulfate particles, *Atmos. Environ.*, 19(5), 819–825, 1985.

5 Stokes, R. H. and Robinson, R. A.: Interactions in aqueous nonelectrolyte solutions, I. Solute-solvent equilibria, *J. Phys. Chem.*, 70, 2126–2130, 1966.

Topping, D. O., McFiggans, G. B., and Coe, H.: A curved multi-component aerosol hygroscopicity model framework: Part 2 – Including organic compounds, *Atmos. Chem. Phys.*, 5, 1223–1242, 2005,

10 <http://www.atmos-chem-phys.net/5/1223/2005/>.

Yu, S., Dennis, R., Roselle, S., Nenes, A., Walker, J., Eder, B., Schere, K., Swall, J., and Rorbarge, W.: An assessment of the ability of three-dimensional air quality models with current thermodynamic equilibrium models to predict aerosol NO_3^- , *J. Geophys. Res.*, 110, D07S13, doi:10.1029/2004JD004718, 2005.

15 Wexler, A. S. and Clegg, S. L.: Atmospheric aerosol models for systems including the ions H^+ , NH_4^+ , Na^+ , SO_4^{2-} , NO_3^- , Cl^- , Br^- and H_2O , *J. Geophys. Res.*, 107(D14), 4207, doi:10.1029/2001JD000451.593, 2002.

Wexler, A. S. and Seinfeld, J. H.: The distribution of ammonium salts among a size and composition dispersed aerosol. *Atmos. Environ.*, 24A, 1231–1246, 1990.

20 Wexler, A. S. and Seinfeld, J. H.: Second-generation inorganic aerosol model. *Atmos. Environ.*, 25A, 2731–2748, 1991.

Zaveri, R. A., Easter, R. C., and Peters, L. K.: A computationally efficient Multi-component Equilibrium Solver for Aerosols (MESA), *J. Geophys. Res.*, 110, D24203, doi:10.1029/2004JD005618, 2005.

25 Zhang, Y., Seigneur, C., Seinfeld, J. H., Jacobson, M. Z., Clegg, S. L., and Binkowski, F.: A comparative review of inorganic aerosol thermodynamic equilibrium modules: similarities, differences, and their likely causes, *Atmos. Environ.*, 34, 117–137, 2000.

Table 1. Description of the parameterization and methods in EQUISOLV II and EQSAM3.

	EQUISOLV II	EQSAM3
Binary activity coefficients	A number of measurements, Pitzer's method and Harned and Owen's method ^a	Derived as a function of temperature, relative humidity and solubility of chemical compounds ^b
Multi-component activity coefficients	Bromley (Bromley, 1973)	N/A
Water activity	ZSR ^c	Osmotic pressure additivity ^c
DRH/CRH	Prescribed based on a number of laboratory measurements for electrolytes at 298 K	Derived as a function of the solubility of chemical compound and temperature
MDRH	N/A ^d	Derived as a function of the solubility of chemical compounds and temperature
Solution method	Iterative chemical equilibrium and mass-flux iteration techniques	Analytical solution according to the solutes precipitation order (non-iterative)
System solved in this study	$H^+ - NH_4^+ - Na^+ - Ca^{2+} - Mg^{2+} - K^+ - OH^- - NO_3^- - SO_4^{2-} - Cl^- - CO_3^{2-}$	$H^+ - NH_4^+ - Na^+ - Ca^{2+} - Mg^{2+} - K^+ - OH^- - NO_3^- - SO_4^{2-} - Cl^- - CO_3^{2-}$
Reference	Jacobson et al. (1996), Jacobson (1999)	Metzger and Lelieveld (2007)

^a Pitzer's method (Pitzer and Mayorga, 1973) and a number of measurements (Table B.9, Jacobson, 2005) are adopted to predict the mean binary solute activity coefficients at 298.15 K while the temperature dependence of the coefficients is predicted using the Harned and Owen (1958) method.

^b Mean ion-pair activity coefficients are needed only for volatile compounds (i.e., NH_4NO_3 and NH_4Cl) in EQSAM3.

^c EQUISOLV II uses the so-called Zdanovskii-Stokes-Robinson (ZSR, Stokes and Robison, 1966) mixing rule to estimate liquid water content at equilibrium, which is explained by the additivity of osmotic pressures (Metzger and Lelieveld, 2007) and applied as this in EQSAM3.

^d The MDRH in EQUISOLV II is not a function of chemical composition and temperature but can be inferred by solving the solid-liquid equilibrium reactions at various RH (Zaveri et al., 2005).

A comparison of water uptake

L. Xu et al.

Title Page

Abstract

Introduction

Conclusions

References

Tables

Figures

◀

▶

◀

▶

Back

Close

Full Screen / Esc

Printer-friendly Version

Interactive Discussion



A comparison of water uptake

L. Xu et al.

Table 2. List of solubility and corresponding DRH of major solid compounds in EQSAM3 at a temperature 298 K.

	Solubility (%) ^a	DRH (298K) ^b
(NH ₄) ₂ SO ₄	36.66 (43.31)	0.7997 (0.7980)
NH ₄ HSO ₄	64.72 (76.00)	0.4000 (0.3999)
NH ₄ NO ₃	56.83 (68.05)	0.6183 (0.6067)
NH ₄ Cl	23.53 (28.34)	0.7710 (0.7659)
Na ₂ SO ₄	39.86 (21.94)	0.8420 (0.9390)
NaHSO ₄	76.57 (90.00)	0.5200 (0.9285)
NaNO ₃	40.98 (47.70)	0.7450 (0.7476)
NaCl	22.66 (26.47)	0.7528 (0.7540)

^a The number inside of the parenthesis is that from Table 1 and 2 of Metzger and Lelieveld (2007) while the number outside is the deduced solubility used in this study.

^b The DRH inside of the parenthesis is that derived from the solubility of solutes looked up from the Handbook of Chemistry and Physics (Metzger and Lelieveld, 2007), while the value outside the parentheses is the DRH used in this study.

Title Page

Abstract

Introduction

Conclusions

References

Tables

Figures

◀

▶

◀

▶

Back

Close

Full Screen / Esc

Printer-friendly Version

Interactive Discussion



A comparison of water uptake

L. Xu et al.

Title Page

Abstract

Introduction

Conclusions

References

Tables

Figures

◀

▶

◀

▶

Back

Close

Full Screen / Esc

Printer-friendly Version

Interactive Discussion



Table 3. List of 20 conditions for model simulations^a.

Sulfate condition	Case No.	$\frac{t_{\text{NH}_4}}{t_{\text{SO}_4}}$	$\frac{t_{\text{NO}_3}}{t_{\text{SO}_4}}$	$\frac{t_{\text{NaCl}}}{t_{\text{SO}_4}}$	$\frac{t_{\text{K}}}{t_{\text{SO}_4}}$	$\frac{t_{\text{Ca}}}{t_{\text{SO}_4}}$	$\frac{t_{\text{Mg}}}{t_{\text{SO}_4}}$
Sulfate rich	1(2)	1.0	1.0	0	0	0	0
	2(8)	1.5	3.0	0	0	0	0
	3(10)	0.5	1.0	0.5	0	0	0
	4	0.5	1.0	0.5	0.04	0.02	0.01
	5	1.5	3.0	0	0.04	0.02	0.01
Sulfate neutral	6(14)	2.0	1.0	0	0	0	0
	7(15)	1.5	0.33	0.5	0	0	0
	8(17)	1.5	3.0	0.5	0	0	0
	9	1.5	0.33	0.4	0.04	0.02	0.01
	10	1.5	3.0	0.4	0.04	0.02	0.01
Sulfate poor	11(5)	4.0	1.0	0	0	0	0
	12(9)	4.0	3.0	0	0	0	0
	13(13)	2.0	1.0	0.5	0	0	0
	14(14)	4.0	1.0	0.5	0	0	0
	15(20)	4.0	1.0	2.0	0	0	0
	16	2.0	1.0	0.5	0.04	0.02	0.01
	17	4.0	1.0	0.5	0.04	0.02	0.01
	18	4.0	1.0	2.0	0.04	0.02	0.01
	19	4.0	1.0	0	0.04	0.02	0.01
	20	4.0	3.0	0	0.04	0.02	0.01

^a The particulate sulfate concentration is fixed as $20 \mu\text{g m}^{-3}$ for all cases. The concentration of other aerosol components is listed as molar ratio with respect to the particulate sulfate concentration. Simulations under each set of initial compositions were conducted for 10, 20, 30, 40, 50, 60, 70, 80, 90 and 95% relative humidity at a temperature 298.15 K. The case numbers in the parenthesis refer to the cases in the study by Zhang et al. (2000).

A comparison of water uptake

L. Xu et al.

Table 4. Relative difference as well as linear regression slope with its 95% confidence interval of total particulate matter (PM) and aerosol water (AW) between EQSAM3 and EQUISOLV II for three sulfate regimes at 298.15 K under all RH conditions shown in Fig. 1. “Rich” stands for the sulfate rich regime (i.e., cases 1–5); “Neutral” stands for the sulfate neutral regime (i.e., cases 6–10); “Poor” stands for the sulfate poor regime (i.e., cases 11–20); “All” stands for the conditions including all three sulfate regimes.

Sulfate regime	AW		PM	
	Rel. Diff. (%)	Reg. Slope	Rel. Diff. (%)	Reg. Slope
Rich	39.38	0.91±0.05	−2.02	0.42±0.09
Neutral	−29.87	0.75±0.07	−3.59	0.02±0.045
Poor	−28.06	0.79±0.06	15.42	0.54±0.08
All	−3.79	0.79±0.03	6.30	0.89±0.04

[Title Page](#)
[Abstract](#)
[Introduction](#)
[Conclusions](#)
[References](#)
[Tables](#)
[Figures](#)
[Back](#)
[Close](#)
[Full Screen / Esc](#)
[Printer-friendly Version](#)
[Interactive Discussion](#)


A comparison of water uptake

L. Xu et al.

Table 5. Total Particulate matter (PM) concentration predicted at 298.15 K and RH 30% under all conditions. The value in parentheses in the column for EQUISOLV II is the model-average PM concentration from Zhang et al. (2000) for the reference. The value in parentheses in the column for EQSAM3 is the PM concentration using the DRH-dependent neutralization order. The relative difference is defined as the normalized difference in the PM concentration predicted by EQSAM3 and EQUISOLV II. The value in the parentheses is the difference corresponding to the DRH-dependent neutralization order while that outside the parentheses corresponds to the prescribed neutralization order (specified by the Hofmeister series) in EQSAM3.

Condition	PM concentrations ($\mu\text{g m}^{-3}$)		Relative difference (%)
	EQSAM3	EQUISOLV II	
1	23.69 (32.11)	23.69 (23.3)	0.00 (35.54)
2	25.33 (37.96)	25.32 (25.1)	0.04 (49.92)
3	24.30 (35.42)	24.30 (21.5)	0.00 (45.76)
4	24.21 (36.68)	24.81	-2.42 (47.84)
5	25.24 (39.3)	25.97	-2.81 (51.33)
6	26.97 (36.05)	26.96 (26.8)	0.04 (33.72)
7	27.57 (35.24)	27.57 (25.6)	0.00 (27.82)
8	27.57 (48.08)	27.57 (24.9)	0.00 (74.39)
9	27.04 (35.01)	27.77	-2.63 (26.07)
10	27.04 (47.34)	27.77	-2.63 (70.47)
11	39.04 (39.04)	27.51 (26.9)	41.91 (41.91)
12	47.14 (60.75)	39.21 (40.5)	20.22 (54.93)
13	32.45 (44.78)	28.01 (27.4)	15.85 (59.87)
14	42.08 (48.28)	28.01 (30.5)	50.23 (72.37)
15	51.18 (66.39)	40.00 (40.6)	27.95 (65.98)
16	33.86 (45.84)	28.32	19.56 (61.86)
17	41.43 (49.24)	28.98	42.96 (69.91)
18	51.14 (67.36)	40.87	25.13 (64.82)
19	38.39 (40.38)	28.06	36.81 (43.91)
20	48.32 (61.73)	40.66	18.84 (51.82)

[Title Page](#)
[Abstract](#)
[Introduction](#)
[Conclusions](#)
[References](#)
[Tables](#)
[Figures](#)
[I◀](#)
[▶I](#)
[◀](#)
[▶](#)
[Back](#)
[Close](#)
[Full Screen / Esc](#)
[Printer-friendly Version](#)
[Interactive Discussion](#)


A comparison of water uptake

L. Xu et al.

Table 6. Comparison between modeled and observed concentrations of gas and particulate phase ammonium, nitrate and chloride by EQSAM3 (EQ3) and EQUISOLV II (EQ2) as well as the model predicted concentrations of total particulate matter, solid particulate matter and aerosol associated water. The observational data are from the MINOS campaign (Metzger et al., 2006).

Variable	Concentration ^a ($\mu\text{g m}^{-3}$)			Bias ^a ($\mu\text{g m}^{-3}$)		Percentage within a factor of 2 (%) ^b		Percentage within a factor of 1.5 (%) ^b	
	EQ3	EQ2	Obs.	EQ3	EQ2	EQ3	EQ2	EQ3	EQ2
NH_4^+ (p)	2.14±0.93	1.65±0.77	2.20±1.62	-0.06±0.92	-0.55±1.05	90.71	90.16	72.13	68.31
NH_3 (g)	0.68±0.91	1.14±1.08	0.77±0.69	-0.10±0.80	0.36±0.91	36.07	53.01	21.31	36.07
NO_3^- (p)	0.82±0.58	0.04±0.10	0.09±0.04	0.73±0.59	-0.05±0.10	1.64	10.38	1.09	6.56
HNO_3 (g)	0.61±0.58	1.40±0.79	1.33±0.78	-0.72±0.59	0.07±0.10	20.22	100.00	18.58	98.91
Cl^- (p)	0.51±0.51	0.03±0.11	0.06±0.07	0.45±0.53	-0.03±0.11	8.20	10.93	4.92	8.20
HCl(g)	2.03±1.41	2.46±1.45	2.42±1.47	-0.39±0.53	0.03±0.11	91.26	91.26	61.75	91.26
PM	8.36±3.35	6.76±2.79	9.62±3.57	-1.26±1.48	-2.86±1.69	100.0	91.26	89.62	65.57
PM(s)	6.91±4.20	4.13±4.13	-	-	-	-	-	-	-
H_2O (aq)	2.41±4.99	3.29±4.26	-	-	-	-	-	-	-

^a The value of the concentration and bias is given as the mean \pm standard deviation and the bias is defined as the absolute difference between the model predictions and the observations.

^b The percentages of the model predicted points that are within a factor of 1.5 or 2.0 of the observations. The total number of samples during the MINOS campaign was 183.

[Title Page](#)
[Abstract](#)
[Introduction](#)
[Conclusions](#)
[References](#)
[Tables](#)
[Figures](#)
[I◀](#)
[▶I](#)
[◀](#)
[▶](#)
[Back](#)
[Close](#)
[Full Screen / Esc](#)
[Printer-friendly Version](#)
[Interactive Discussion](#)


A comparison of
water uptake

L. Xu et al.

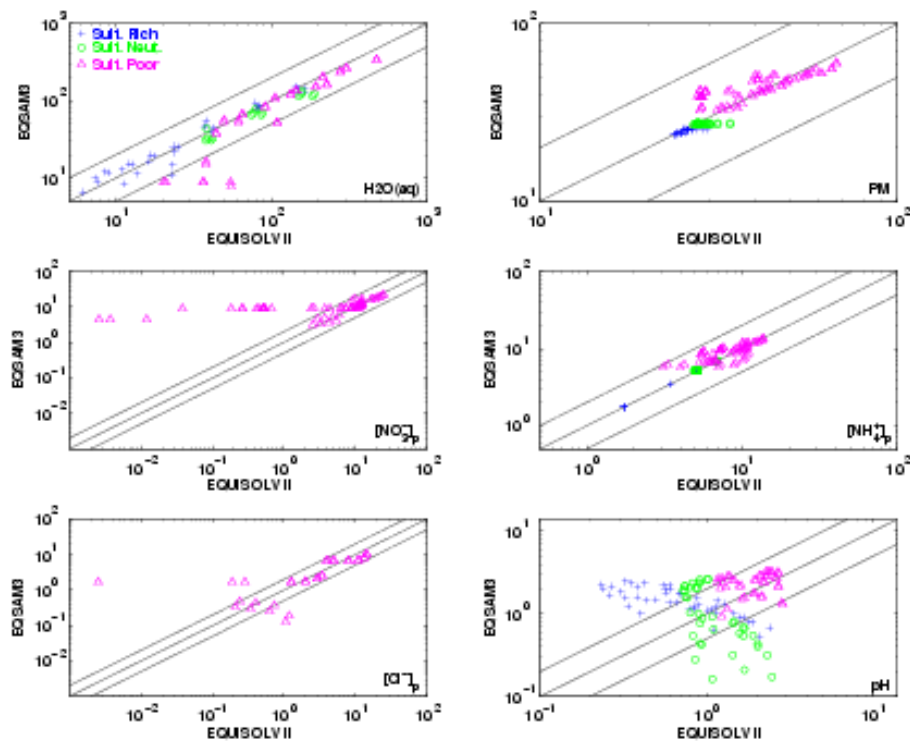


Fig. 1. Scatter plots of aerosol water ($\text{H}_2\text{O}(\text{aq})$), total particulate matter (PM), particulate NO_3^- ($[\text{NO}_3^-]_p$), particulate NH_4^+ ($[\text{NH}_4^+]_p$), particulate Cl^- ($[\text{Cl}^-]_p$), and potential of hydrogen (pH) predicted by EQSAM3 and EQUISOLV II based on the 200 initial conditions specified in Table 3 at a temperature 298.15 K. The black dashed lines are the 1:2, 1:1, 2:1 lines, respectively. The units are $\mu\text{g m}^{-3}$. The concentration is shown using a logarithm scale.

Title Page

Abstract

Introduction

Conclusions

References

Tables

Figures

◀

▶

◀

▶

Back

Close

Full Screen / Esc

Printer-friendly Version

Interactive Discussion



A comparison of water uptake

L. Xu et al.

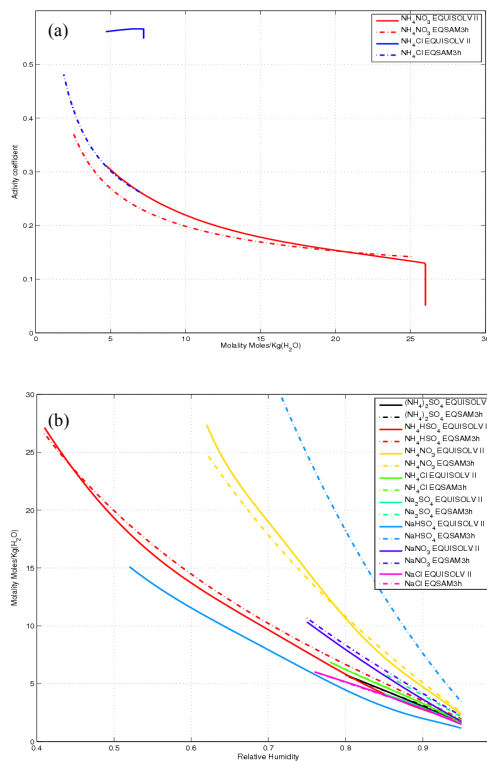


Fig. 2. (a) mean binary activity coefficients of NH_4NO_3 and NH_4Cl as a function of molality; (b) molality for several electrolytes at a temperature 298.15 K as a function of water activity (i.e., RH with a 0–1 scale).

Title Page

Abstract

Introduction

Conclusions

References

Tables

Figures

◀

▶

◀

▶

Back

Close

Full Screen / Esc

Printer-friendly Version

Interactive Discussion



A comparison of
water uptake

L. Xu et al.

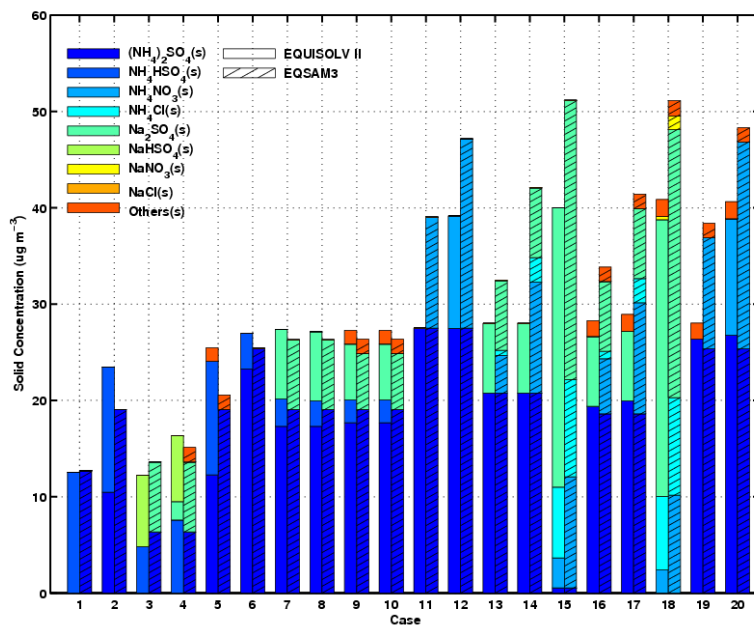


Fig. 3. The concentrations of major solid compounds predicted by EQSAM3 and EQUISOLV II at an RH of 30% and a temperature of 298.15 K for the 20 cases listed in Table 3.

Title Page

Abstract

Introduction

Conclusions

References

Tables

Figures

◀

▶

◀

▶

Back

Close

Full Screen / Esc

Printer-friendly Version

Interactive Discussion



**A comparison of
water uptake**

L. Xu et al.

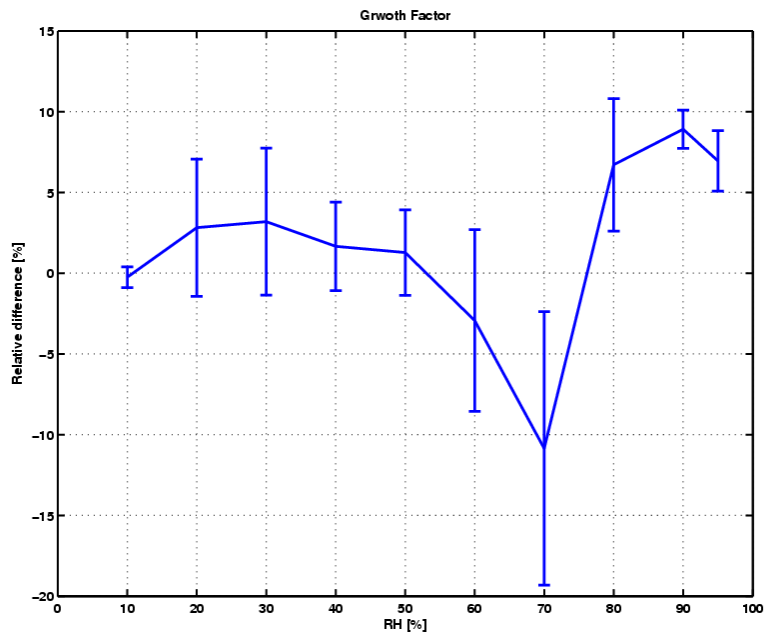


Fig. 4. Relative difference in the growth factor between EQSAM3 and EQUISOLV II for all 200 cases in Table 3 as a function of RH at a temperature 298.15 K. The error bars indicate the range of values for different cases.

[Title Page](#)[Abstract](#)[Introduction](#)[Conclusions](#)[References](#)[Tables](#)[Figures](#)[I◀](#)[▶I](#)[◀](#)[▶](#)[Back](#)[Close](#)[Full Screen / Esc](#)[Printer-friendly Version](#)[Interactive Discussion](#)

A comparison of
water uptake

L. Xu et al.

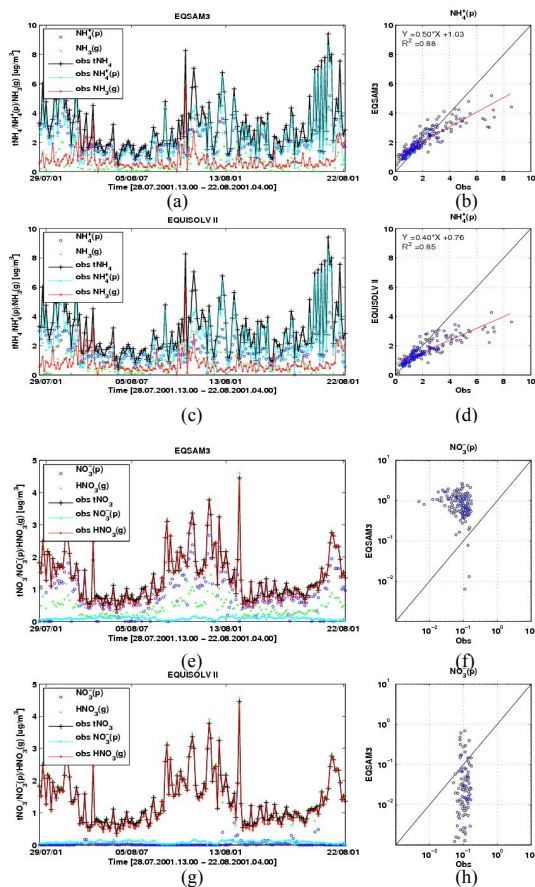


Fig. 5. Time series of the EQSAM3 and EQUISOLV II predictions and observations for $\text{NH}_4^+(\text{p})$, $\text{NH}_3(\text{g})$, tNH_4 , $\text{NO}_3^-(\text{p})$, $\text{HNO}_3(\text{g})$, tNO_3 during the period of the MINOS campaign. The red line in the panels at the right is a linear fit to the data.

Title Page

Abstract

Introduction

Conclusions

References

Tables

Figures

◀

▶

◀

▶

Back

Close

Full Screen / Esc

Printer-friendly Version

Interactive Discussion



A comparison of
water uptake

L. Xu et al.

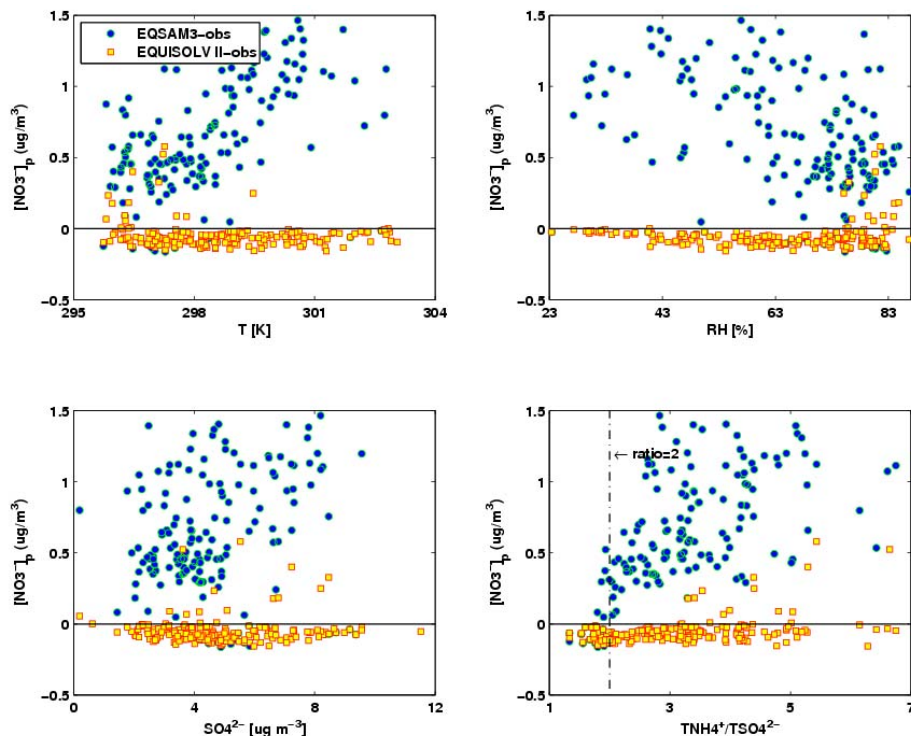


Fig. 6. The difference between the modeled and observed concentrations of NO_3^- as a function of temperature, RH, SO_4^{2-} concentration, and the molar ratio of TNH_4^+ to TSO_4^{2-} during the MINOS campaign.

[Title Page](#)[Abstract](#)[Introduction](#)[Conclusions](#)[References](#)[Tables](#)[Figures](#)[◀](#)[▶](#)[◀](#)[▶](#)[Back](#)[Close](#)[Full Screen / Esc](#)[Printer-friendly Version](#)[Interactive Discussion](#)

A comparison of
water uptake

L. Xu et al.

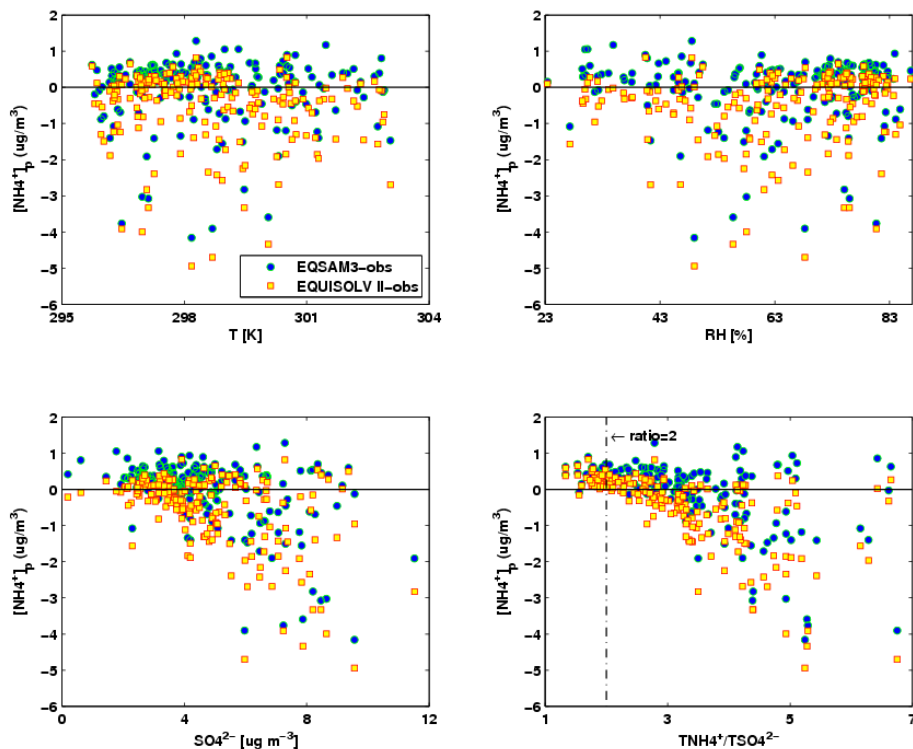


Fig. 7. The difference between the modeled and observed concentrations of NH_4^+ as a function of temperature, RH, SO_4^{2-} concentration, and the molar ratio of TNH_4^+ to TSO_4^{2-} during the MINOS campaign.

[Title Page](#)[Abstract](#)[Introduction](#)[Conclusions](#)[References](#)[Tables](#)[Figures](#)[◀](#)[▶](#)[◀](#)[▶](#)[Back](#)[Close](#)[Full Screen / Esc](#)[Printer-friendly Version](#)[Interactive Discussion](#)

**A comparison of
water uptake**

L. Xu et al.

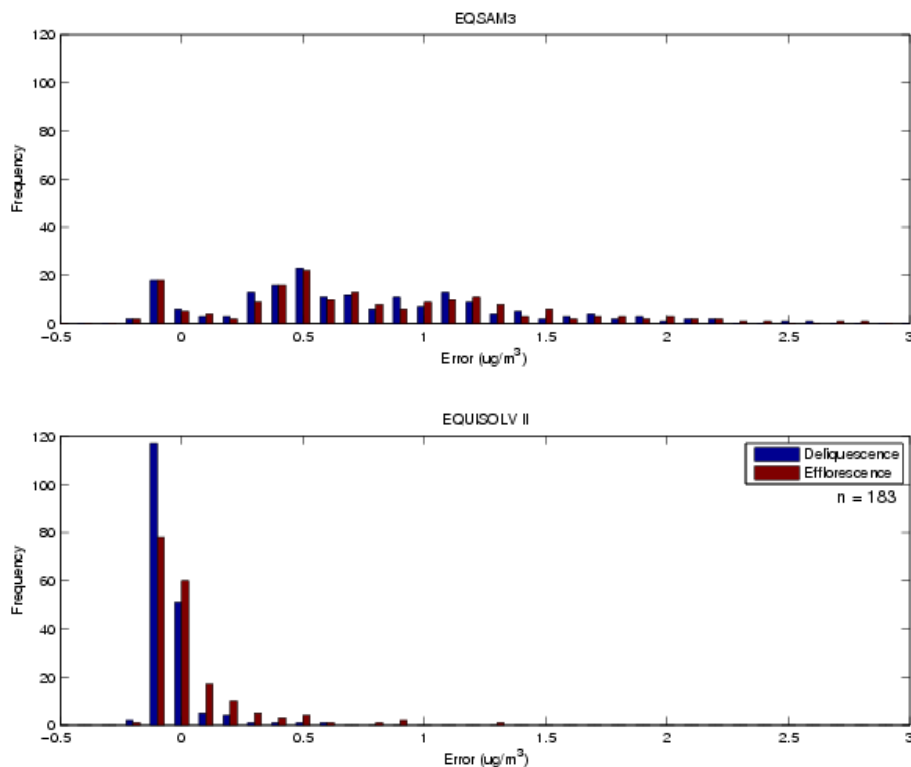


Fig. 8. Error distributions of aerosol nitrate assuming different equilibrium states (deliquescence vs. efflorescence) of the particles during the MINOS campaign. Errors are calculated as the predicted minus the observed values of aerosol nitrate. The number of samples was 183.

[Title Page](#)[Abstract](#)[Introduction](#)[Conclusions](#)[References](#)[Tables](#)[Figures](#)[I◀](#)[▶I](#)[◀](#)[▶](#)[Back](#)[Close](#)[Full Screen / Esc](#)[Printer-friendly Version](#)[Interactive Discussion](#)